

# The Interchromatin Compartment Participates in the Structural and Functional Organization of the Cell Nucleus

Thomas Cremer,\* Marion Cremer, Barbara Hübner, Asli Silaharoglu, Michael Hendzel, Christian Lanctôt, Hilmar Strickfaden,\* and Christoph Cremer\*

This article focuses on the role of the interchromatin compartment (IC) in shaping nuclear landscapes. The IC is connected with nuclear pore complexes (NPCs) and harbors splicing speckles and nuclear bodies. It is postulated that the IC provides routes for imported transcription factors to target sites, for export routes of mRNA as ribonucleoproteins toward NPCs, as well as for the intranuclear passage of regulatory RNAs from sites of transcription to remote functional sites (IC hypothesis). IC channels are lined by less-compacted euchromatin, called the perichromatin region (PR). The PR and IC together form the active nuclear compartment (ANC). The ANC is co-aligned with the inactive nuclear compartment (INC), comprising more compacted heterochromatin. It is postulated that the INC is accessible for individual transcription factors, but inaccessible for larger macromolecular aggregates (limited accessibility hypothesis). This functional nuclear organization depends on still unexplored movements of genes and regulatory sequences between the two compartments.

inseparably connected with their functional tasks at all levels, from molecules to genes, chromatin domains (CDs), chromosome territories, and the functional nuclear organization at large.

The “top-down” approach to explore nuclear structure and function started in the nineteenth century with the discovery of the cell nucleus, its indirect division with the formation of mitotic chromosomes, and the first description of chromatin.<sup>[12–14]</sup> The “bottom up” followed in the twentieth century culminating with the discovery that chromosomes carry a text written by evolution into immensely long DNA molecules. The direct visualization of specific genes located on chromosomes became possible, when Mary Pardue and Joseph Gall invented a method for the molecular hybridization of DNA probes to the DNA of cytological preparations.<sup>[15]</sup> For reviews, see refs. [16,17].


## 1. Introduction

During the last two decades, the compartmentalized structure of the cell nucleus and packaging of its genome has become a key issue for the understanding of nuclear functions.<sup>[1–8]</sup> Methodological progress has now reached a state where we are witnessing the rise of a new research field, called the 4D nucleome.<sup>[9–11]</sup> It has become evident that the structural organization of nuclei is

In 1968, David Comings published a seminal paper about “The Rationale for an Ordered Arrangement of Chromatin in the Interphase Nucleus” where he argued for a spaghetti-like assembly of chromatin fibers possibly connected to the nuclear pore complexes (NPCs).<sup>[18,19]</sup> During the 1960s and 1970s, the cell nucleus was still widely conceived as a chemical reaction vial with proteins and RNAs diffusing in the nuclear sap in a

Prof. T. Cremer, Dr. M. Cremer, B. Hübner<sup>[+]</sup>  
Anthropology and Human Genomics, Department of Biology II  
Ludwig-Maximilians University (LMU)  
Biocenter, Grosshadernerstr. 2, 82152 Martinsried, Germany  
E-mail: Thomas.Cremer@lrz.uni-muenchen.de

Prof. A. Silaharoglu  
Department of Cellular and Molecular Medicine Faculty of Health and  
Medical Sciences  
University of Copenhagen  
Nørre Alle 14, Byg. 18.03, 2200 Copenhagen N, Denmark  
Prof. M. Hendzel, Dr. H. Strickfaden  
Department of Oncology, Cross Cancer Institute  
University of Alberta  
11560 University Avenue, Edmonton, Alberta T6G 1Z2, Canada  
E-mail: hilmar@ualberta.ca

 The ORCID identification number(s) for the author(s) of this article can be found under <https://doi.org/10.1002/bies.201900132>

<sup>[+]</sup>Present address: Institute of Structural Biology (NISB), School of Biological Sciences, Nanyang Technological University, 50 Nanyang Avenue, Singapore 639798, Singapore

© 2020 The Authors. *BioEssays* published by WILEY Periodicals, Inc. This is an open access article under the terms of the Creative Commons Attribution-NonCommercial License, which permits use, distribution and reproduction in any medium, provided the original work is properly cited and is not used for commercial purposes.

DOI: 10.1002/bies.201900132

Dr. C. Lanctôt  
Integration Santé  
1250 Avenue de la Station local 2-304, Shawinigan, Québec G9N 8K9, Canada

Prof. C. Cremer  
Institute of Molecular Biology (IMB) Ackermannweg 4, 55128 Mainz, Germany, and Institute of Pharmacy & Molecular Biotechnology (IPMB) University Heidelberg  
Im Neuenheimer Feld 364, 69120 Heidelberg, Germany  
E-mail: C.Cremer@imb-mainz.de; Cremer@bmm.uni-heidelberg.de

largely unrestricted way. Only a few molecular biologists became already interested in problems of 3D genome organization during the 1970s.<sup>[20]</sup> Francis Crick, one of the most influential advocates of the bottom-up approach, asked “How much does the 3D structure of the eukaryotic genome matter for expression, compared to the 1D structure?”<sup>[21]</sup> “The methods of studying 3D structures with precision are far more difficult than the methods available for sequencing DNA. Thus, if it turns out [...] that the 3D structure is not merely a packing device needed mainly for mitosis but is also of primary importance for gene expression, then [...] we will need a more devious and ingenious plan of attack. Only time can show which alternative is preferred by nature and how difficult the problem will turn out to be.” In a lecture delivered in 1977 at the Sixth International Chromosome Conference in Helsinki, Crick acknowledged the advance of the new chromosome banding techniques in genetic mapping and the clinical importance to identify all human chromosomes and larger deletions and translocations, but reminded his audience of cytogeneticists (one of the authors of this article [T. Cremer] was among them): “The metaphase chromosome, which is the object of study of many of the conference members, is the dullest form of chromosome: an inert package needed to make orderly mitosis possible. [...] Unfortunately, this is the least rewarding form to study microscopically.”<sup>[22]</sup> Because of the limited resolution of cytological methods, Crick doubted that they could ever make a meaningful contribution to understand the 3D organization of chromosomes. “Evolution, guided by natural selection, must always remain the grandest theme in biology, but if we are to arrive at a deep understanding [...] it is essential (among other things) to know exactly what constitutes a eukaryotic gene.” Crick hoped for possibilities of genetic engineering to obtain biochemically useful amounts of a “pure gene,” and ended his lecture with this statement: “I feel that chromosome workers will ignore these coming advances in molecular biology to their peril. It is not enough, in order to understand the book of Nature, to turn over the pages and look on the pictures. Painful, so it may be, it is necessary to read the text. Only with the assistance of molecular biology this will be possible.”<sup>[22]</sup>

Both top-down and bottom-up strategies must be integrated in the attempt to understand the interplay of structure and function in the most complex organelle of the cell. Sophisticated methods that allow the quantitative description of nuclear landscapes have always been instrumental to identify problems that require a mechanistic explanation, starting with the discovery of mitosis. The study of the nuclear architecture of mammalian rod photoreceptor cells may serve here as another case in point to illustrate this necessity.<sup>[23]</sup> Unexpectedly, a profound difference was detected between the nuclear architecture of rods in mammalian species with a diurnal life and species, which are predominantly active at night, dusk and dawn. Rods of diurnal mammals possess the conventional architecture found in nearly all eukaryotic cells, with most heterochromatin situated at the nuclear periphery and euchromatin residing toward the nuclear interior. In contrast, in crepuscular species, compact heterochromatin expands in the nuclear center, whereas less-compacted euchromatin lines the nuclear border. This inverted pattern forms by remodeling of the conventional one during terminal differentiation of rods. The underlying mechanism apparently evolved

because of a selective advantage: Inverted rod nuclei act as collecting lenses and allow visual orientation in a low-light environment. This example demonstrates the profound potential for major modifications of nuclear architecture enforced by selective pressure and also how primarily descriptive top-down strategies pave the way to the identification and further exploration of new mechanisms.<sup>[24]</sup>

The discovery of nucleosomes in the 1970s marked the beginning of a major change in our understanding of chromatin's functional capacities.<sup>[25–28]</sup> The enigma of the nucleosome's functional roles beyond DNA packaging was lifted, when it was discovered that tightly controlled epigenetic modifications contribute directly to regulation of both chromatin structure and transcription, prompting a still ongoing change of paradigm in our understanding of genetic and environmental interactions. Nucleosomes form  $\approx 10$  nm thick chromatin fibers. The folding of these fibers into a hierarchy of higher-order chromatin structures in nuclei of living cells has remained an intensely debated problem.<sup>[29]</sup> At approximately 2 m before (G1) and 4 m after DNA replication (G2 and mitosis), the DNA molecules contained within a diploid mammalian cell nuclei appear immensely long, given that they are packaged within diploid mammalian cell nuclei with typical diameters of between 5 and 15  $\mu\text{m}$ . However, packaging a quantity of about 6000 megabase pairs (Mbp) wrapped around up to 30 million nucleosomes in a diploid mammalian cell nucleus leaves still plenty of space for an interchromatin compartment (IC) crowded with non-histone proteins, RNAs, and functional macromolecular aggregates. This article emphasizes the perspective that the IC represents a nuclear compartment with its own functions which co-evolved together with the “crumpled” organization of chromatin.<sup>[30]</sup>

## 2. The ANC-INC Model: Functional Nuclear Organization Based on co-Aligned Active and Inactive Compartments

The ANC-INC model<sup>[31]</sup> is a refined version of the chromosome territory–interchromatin compartment (CT-IC) model.<sup>[32]</sup>

Microscopic evidence for the ANC-INC model (**Figure 1**) described below demonstrates that chromatin domains (CDs) are pervaded by a branched contiguous network of channels with direct contacts to NPCs. In a broad sense an interchromatin space forms by necessity, when chromatin loops are organized into compact CDs. By our use of the term interchromatin compartment, we emphasize our expectation that the IC has functional properties of its own. Expanded regions of the IC, called IC lacunas, harbor a variety of nuclear bodies.<sup>[31]</sup> Movements of splicing speckles are a telling example for the capability of functional macromolecular aggregates to move along IC channels whose width appears to be adjustable to functional needs.<sup>[33,34]</sup>

The IC is characterized by a very low average DNA density, likely resulting from relatively sparse chromatin- or even naked DNA loops (**Figure 1A,B**) penetrating into the IC interior from lining CDs. Arguably, specific types of proteins and regulatory RNAs enrich within the IC and form larger functional aggregates for transcription, splicing, replication, and repair either directly within the IC or in its lining, functionally competent

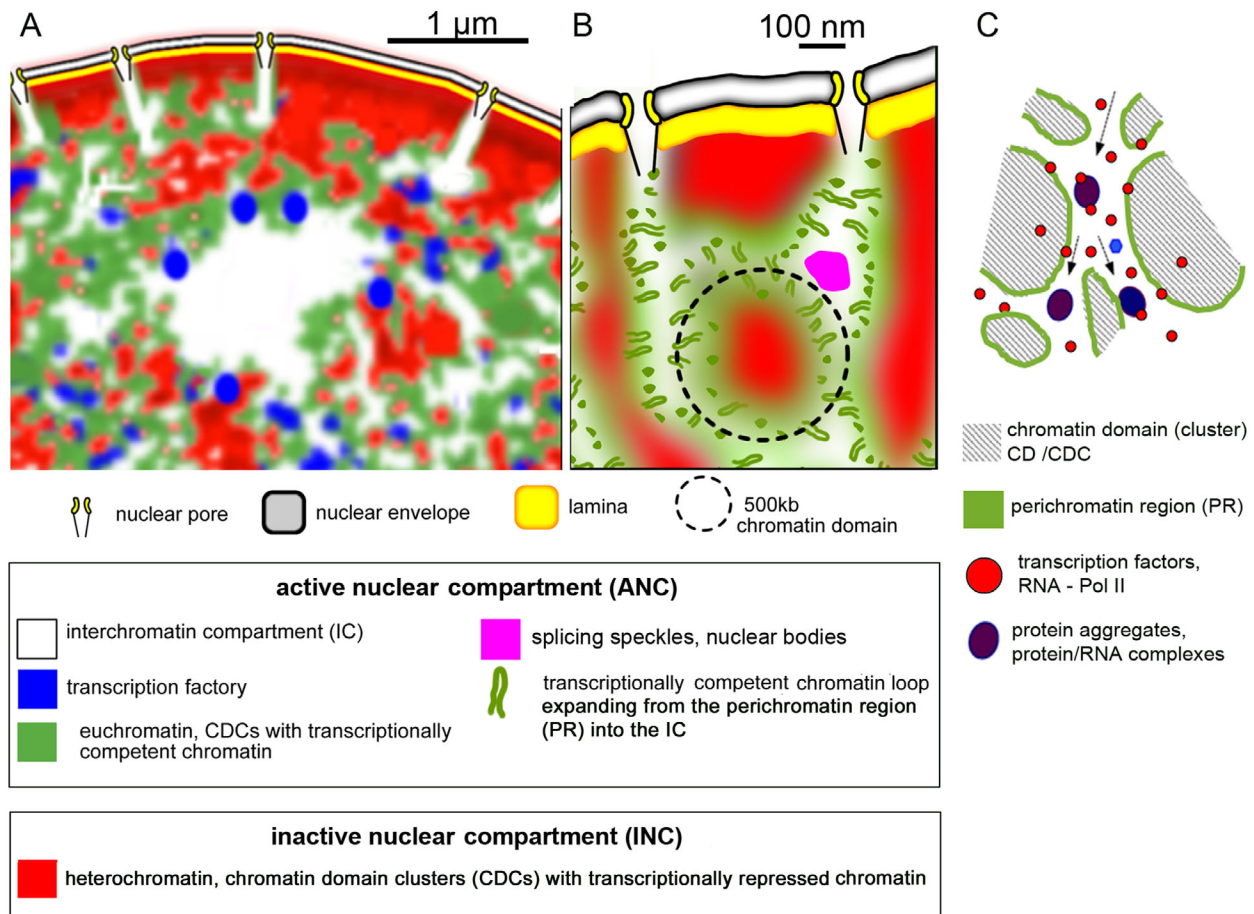


**Figure 1.** ANC-INC network model. A) The scheme exemplifies the topographical relation of the spatially co-aligned active and inactive nuclear compartments (ANC and INC). Shown are several chromatin domain clusters (CDCs) of a chromosome territory (CT) associated with the nuclear envelope. The ANC is composed of two parts: first, a 3D-channel network, called the interchromatin compartment (IC, white), which starts at nuclear pores and forms a contiguous branched 3D network throughout the nuclear interior containing proteins, RNAs, and macromolecular aggregates, such as nuclear bodies and speckles (blue); second, easily accessible, transcriptionally competent chromatin (green), called the perichromatin region (PR), which forms the borders of the IC channels. The PR is enriched in regulatory and coding sequences of active genes and represents the nuclear subcompartment, where most of the transcription, splicing of primary transcripts, as well as transcription of regulatory RNAs takes place. Accordingly, the PR is also enriched in epigenetic marks for transcriptionally competent chromatin, as well as RNAP II and transcription factories. In contrast, more compact chromatin located remote from IC channels can be attributed to the INC (red). It is enriched in epigenetic marks for low or silent transcriptional activity (adapted with permission.<sup>[35]</sup> Copyright 2014, Informa UK Limited). B) ANC/INC topography at somewhat higher resolution with small chromatin loops invading the IC channels. A dotted circle denotes a CD with a DNA content of  $\approx 500$  kbp. In contrast to the model view in (A) where the entire chromatin of a CD lining IC channels may be transcriptionally competent, here this competence is restricted to the periphery of a CD (encircled) (adapted with permission.<sup>[31]</sup> Copyright 2015, Federation of European Biochemical Societies). C) This cartoon (adapted with permission.<sup>[36]</sup> Copyright 2017, Springer Nature) illustrates essentials of the IC hypothesis. CDs and CDCs are represented as gray entities, the PR is depicted as a green contour at CD/CDC borders. Proteins, which enter the IC channel system through nuclear pores, such as transcription factors (TFs), RNAP II and other functional or architectural proteins, are indicated as red dots. It is assumed that individual macromolecules may be specifically enriched within IC channels. They are able to enter the interior of compact chromatin, although their mobility may be considerably more constrained within CDs constituting the INC than within the IC and PR. In contrast, aggregations of proteins and protein/RNA complexes are restricted to the ANC, but fully excluded from the INC. In the diffusion mode, macromolecules are driven by Brownian motion. Arrows suggest a component of a seemingly directed movement, which could result from concentration gradients of macromolecules and/or the streaming of fluid within IC channels or other physicochemical mechanisms.

chromatin, the perichromatin region (PR).<sup>[37–40,42]</sup> The PR is enriched with epigenetic marks for transcriptionally competent chromatin and RNA Polymerase II (RNAPII)<sup>[31]</sup> and serves as the major site of transcription and likely also for the replication of DNA/chromatin as well as repair processes needed for the maintenance of genome integrity.<sup>[40]</sup> Actively transcribed DNA regions with a high-density of RNA polymerase II form transcription hot zones around nuclear speckles.<sup>[41,43]</sup>

At least for euchromatin, the published literature is full of cartoons, which imply a rather open configuration of chromatin loops. In contrast to an interchromatin space expanding both between and in the interior of open chromatin loops, the concept of the interchromatin compartment implies that chromatin loops and the resulting CDs may be compacted to an extent that the access of macromolecules, such as individual transcription factors and regulatory RNAs, can be largely constrained, while the

access of macromolecular aggregates involved in major nuclear functions is fully excluded.<sup>[44]</sup> Based on this conceptual advance, we propose the following hypotheses.

First, we predict that the IC serves as a system for the import, export and intranuclear distribution system of macromolecules including a) routes for the import and channeled mobility of transcription factors (TFs) and numerous other imported proteins, such as RNA polymerases; b) export routes for mRNA packaged as ribonucleoprotein complexes (mRNPs) toward NPCs; c) routes for the intranuclear distribution of non-coding regulatory RNA sequences transcribed at certain nuclear sites to other remote sites of action enriched in the PR (IC hypothesis) (Figure 1C).

Second, we hypothesize that macromolecular machineries required for transcription, replication, and repair are formed within the ANC and that DNA sequences, located in the INC are inaccessible for macromolecular aggregates (limited accessibility hypothesis). Compelling experimental evidence for or against the IC hypothesis and the limited accessibility hypothesis has not yet been obtained. It is currently unknown to which extent individual macromolecules, such as TFs, are able to explore the interior of individual CDs or whether contacts are restricted to targets exposed at CD surfaces.<sup>[45]</sup>

Third, we argue for dynamic structural and functional interactions between the ANC and INC, including mechanisms for movements of chromatin loops or entire CDs between the two co-aligned compartments (dynamic interactions hypothesis). Such mechanisms should allow to lock genes and regulatory sequences away into the INC for long term silencing but also to move them back into the ANC in case of their physiological or pathological activation. Such mechanisms are also required to move sequences or entire CDs from the INC into ANC for DNA/chromatin replication or for repair of DNA damage. CDs carrying genes and regulatory sequences involved in rapid, ongoing changes of expression, or transcriptional bursts may be permanently located in the ANC. In contrast, long-term or permanently inactive genes may be embedded within the highly compacted, facultative heterochromatin of the INC together with inactive regulatory sequences.<sup>[46,47]</sup> Moreover, the topography and spreading of the IC may change in line with functional requirements.

Analogies can help to emphasize important features of a model without distraction by a multitude of technical vocabulary, as long as we keep their limits in mind. The ANC-INC model of a cell nucleus may be compared with a town (Figure 2A–C). Analogous to a transcription factor (TF) approaching its target DNA, a blind Romeo moves through empty streets and places at night (Figure 2D) or crowded with people during the day (Figure 2E). A detailed explanation of this analogy and its limitations is provided in Box 1.

### 3. Support for the ANC-INC Model with Electron Microscopic Studies

#### 3.1. Evidence Obtained with Transmission and Scanning Electron Microscopy

The invention of electron microscopy (EM) by Ruska and Knoll dates back to the early 1930s.<sup>[78]</sup> Today, the best resolution of

commercially available instruments is in the order of 1 nm. Seminal TEM studies carried out with ultrathin nuclear sections (<100 nm) during the late 1960s and early 1970s laid the foundation for our current understanding of nuclear compartmentalization. The EDTA-regressive staining method invented by Wilhelm Bernhard distinguished between DNA and RNA carrying structures and overcame a drawback of early EM staining protocols that lacked this capability. Using this method, Monneron and Bernhard observed an unexpected complexity of the nuclear architecture with clumps of chromatin pervaded by an interchromatin space, including interchromatin and perichromatin granules, perichromatin fibrils, and coiled bodies.<sup>[79]</sup> In another groundbreaking study, Fakan and Bernhard used cultured monkey kidney cells for pulse-labeling experiments with <sup>3</sup>H-Uridine followed by EM autoradiographic analyses.<sup>[80]</sup> (Figure 3A).

This study first identified a border zone between chromatin clusters and the interchromatin space as the nuclear subcompartment for transcription. Notably, an enrichment of silver grains in this border zone became more prominent with increasing pulse labeling times (2–15 min). In agreement with the suggested role of the ANC and the IC hypothesis, radioactivity was retained in the RNP-containing interchromatin space even after prolonged incubation times followed by an additional chase with cold uridine.<sup>[80]</sup> Numerous further EM autoradiographic studies confirmed the functional role of this perichromatin region (compare Figure 1) as the major nuclear subcompartment for transcription<sup>[81–84]</sup> as well DNA replication<sup>[85,86]</sup> and DNA repair,<sup>[39]</sup> for reviews, see refs. [38,40,42].

Currently, an almost isotropic resolution in the small nanometer range has been achieved with respect to 3D reconstructions of cells and nuclei from ultrathin sections.<sup>[87]</sup> In 3D block face-scanning electron microscopy (BF-SEM), a microtome is integrated into a scanning electron microscope that can slice away ultrathin nuclear sections of  $\approx 25$  nm.<sup>[88]</sup> After each step, an image of the newly created surface is recorded. Combined with specific staining of DNA, this approach demonstrated chromatin aggregations in rat liver cell nuclei together with an extended interchromatin space (Figure 3B). En route toward NPCs, interchromatin channels pervade the peripheral layer of heterochromatin (Figure 3C) with direct access to the nuclear pores (see Sections 4.2 and 4.4).<sup>[89]</sup> Another approach combines SEM with a focused ion beam (FIB) for the sequential removal of sections with a thickness down to 3 nm.<sup>[87]</sup> FIB-SEM can be used for cryo-electron microscopy of vitrified sections with an isotropic resolution of 3–5 nm.<sup>[90]</sup> This approach again provided structural evidence for a contiguous system of IC channels with contacts to NPCs (Figure 3D,E).

#### 3.2. Evidence Obtained with Electron Spectroscopic Imaging

Electron spectroscopic imaging (ESI) has made it possible to map the distribution of individual elements, such as phosphorus and nitrogen.<sup>[91]</sup> Although proteins and nucleic acids contain both elements, they differ profoundly with respect to their nitrogen/phosphorus ratios. The collection of phosphorus and nitrogen maps allows the generation of composite images that readily contrast the chromatin with the interchromatin compartment. This has made it possible to distinguish the



**Figure 2.** The cell nucleus as a town: A) Model of a cell nucleus, adapted with permission.<sup>[48]</sup> Copyright 2000, Begell House Inc., shows the interchromatin compartment (IC) (green) starting at nuclear pores with IC-channels, expanding into wider IC-lacunae in the nuclear interior (scale bar: 5  $\mu$ m). In addition, three chromosome territories (CTs) (red) are drawn arbitrarily on a confocal section through a HeLa cell nucleus with GFP-labeled histones H2B (white); n indicates nucleoli. One CT (bottom) reveals IC-channels expanding between  $\approx$ 1-Mbp chromatin domains (CDs). Another CT (top left) shows CDs composed of  $\approx$ 100-kbp subdomains, pervaded by the finest IC-channels.<sup>[48]</sup> B) Adaptation from Monachium Bavariae with permission of Stadtarchiv München. This Munich city plan from 1613 was drawn by Tobias Volckmer (1586-1659). Gates (arrows), houses, quarters (some arbitrarily marked in red and blue) and pervading streets (some marked in green) correspond to nuclear pores, CDs and CTs. C) Pieter Brueghel the Elder "The fight between carnival and lent" (1559) reproduced with permission from KHM-Museumsverband Wien. D) and E) Adaptations from Brueghel's painting emphasize features analogous to the cell nucleus as a town (for details see Box 1). D) Romeo in search for Juliet stands on the empty market place.<sup>[49]</sup> Since Romeo is blind, he meanders over the empty place (white line). E) Various groups, including a group of carnavalists and drinkers (left) and another of faithful and pious persons (right), dominate the crowded marketplace. For lack of membership, Romeo is excluded from both groups in analogy to factors excluded from phase separated macromolecular aggregates forming in the IC.<sup>[50]</sup>

### Box 1: Romeo in Search of Juliet: How Does a Transcription Factor Find its Target Sequence?

Romeo has entered the town through one of its gates. His search for Juliet emphasizes the need to study this process not in isolation, but in the context of the structural and functional implications of the whole town. When the place and the roads are deserted at night (Figure 2D), his search is only constrained by the buildings lining the market place and branching streets. Since he is blind and has no a priori information about the position of Juliet's house, his ability to recognize her depends on a direct contact. Coming close to her does not suffice. If he fails to establish a close contact, he may move away from her again with little chance to get as close a second time. Without a guide he has no choice but to meander around with random turns (white lines in Figure 2D). Alternatively, he may move or hop along lining house fronts or try both search strategies in combination. Romeo's search can be further complicated, if Juliet changes her position during his search or if she does not show up at the front of her own house, but is hidden somewhere in the interior. In such a case, Romeo must extend his search into the interior of all houses. This search may be impeded by conditions, which hinder or even fully exclude his entrance into the interior of some or all houses.

Several major limitations of our analogy must be emphasized in line with the fact that the space-time properties of a cell nucleus are more complex than the rather rigid architecture of a 16th century town.

First, the search kinetics of a TF for its target site(s) differ profoundly from a single pair of lovers to find each other. It is essential to know precisely how regulatory factors search for and bind to their targets. In contrast to a monogamous love affair of a single Romeo with a single Juliet, a given TF may search for numerous targets involved in the regulation of a set of genes.<sup>[51]</sup> Hundreds or even thousands of TFs can be simultaneously involved in the search for the same few target site(s), speeding up the finding process within a diploid mammalian genome with 6 billion base pairs (1 billion =  $10^9$  bp) before and 12 billion base pairs after DNA replication. Directed movements may help to position CDs and their genes next to each other, when a functional need arises. Whereas we may expect that two human lovers having found each other will stay together for prolonged periods of time, this is not typical with respect to the interaction of macromolecules, where the assembly and disassembly of protein–protein and protein–nuclear acid interactions may take place in seconds.<sup>[52–54]</sup>

Second, a town may be built to some extent at least by design, but the founders (“designers”) of the little Dutch town (Figure 2B) had surely not in mind the desire of many pairs of lovers to find each other. In contrast, from the very beginning to the present day genomes evolved not by design but according to the rules of a Darwinian evolution. Direct or indirect functional interactions of regulatory factors with specific DNA target sites at the right time and right place have been indispensable for genome regulation and thus at least to some part a matter of survival and natural selection. Structure and function of the 4D nucleome in prokaryotes and eukaryotes

co-evolved as inseparable features.<sup>[30]</sup> Possibly, smaller distances between active genes and regulatory sequences located in the nuclear interior have helped to establish functional networks. The evolution of certain structures opens new avenues, but also sets new constraints for the further evolution of a biological system. The nuclear envelope, for example, was a starting point for the further evolution of non-random radial CT arrangements. For reasons that are still not fully understood, the radial arrangement of the chromatin is stably maintained in both cycling and postmitotic cells in a wide range of species, that is, gene poor CTs and chromosome segments, respectively, are preferentially located at the nuclear periphery, while gene dense CTs and segments occupy the nuclear interior territories and segments in the interior.<sup>[55–61]</sup> Arguably, the interior location of gene dense chromatin observed in all cell types with rare exceptions<sup>[23]</sup> results in smaller distances, even when genes are located on different CTs, and may help to establish non-random, functional interactions.

Third, in nuclei of most cell types, CTs are arranged in intimate contact with each other.<sup>[62]</sup> However, important exceptions of this rule have been detected. For example, nuclei with neighboring CTs, fully separated from each other by broad IC channels, have been recognized in stage specific nuclei during bovine preimplantation development<sup>[35]</sup> (see Section 4.2), as well as in diploid cells in a state of premature senescence induced by activated oncogenes,<sup>[63]</sup> or by treatment of normal or cancer cells with certain drugs.<sup>[64–66]</sup> The problem of how neighboring territories may structurally interact with each other, has not yet been settled. Branco and Pombo have proposed chromatin intermingling based on extended, likely 10 nm thick chromatin loops that penetrate from a given CT into its neighbor.<sup>[67]</sup> Alternatively, strings of sequential CDs may penetrate from one CT as “fingerlike” protrusions into its neighbor.<sup>[40,68]</sup> Both possibilities are not mutually exclusive. In any case, the amount of chromatin intermingling between neighboring CTs must be very limited. Otherwise the success of combinatorial labeling schemes with chromosome paint probes to distinguish well demarcated, differentially colored CTs would not have been possible.<sup>[69]</sup> Fourth, unlike a town with a mostly fixed infrastructure, chromatin domains may be understood as entities with liquid drop like properties<sup>[44]</sup> or properties of visco-elastic gels.<sup>[70–72]</sup> Transitions between the two states are likely of major functional importance. The physicochemistry relevant to this situation involves polymer mechanics in macromolecular crowding conditions.<sup>[50]</sup> Furthermore, in contrast to the rather rigid and stable geometry of a town's quarters and buildings, the 4D geometry of CTs and CDs may change within a short time. CDs are moving continuously at small scales ( $<1 \mu\text{m}$ )<sup>[73]</sup> and may change their compaction.<sup>[74,75]</sup> Large-scale positional changes of entire CTs were reported in nuclei of serum-starved or senescent fibroblast cells and during terminal differentiation of rod cells.<sup>[23,76,77]</sup> In proliferating cells, neighborhood arrangements of individual chromosomes can change profoundly during mitosis.<sup>[73]</sup>

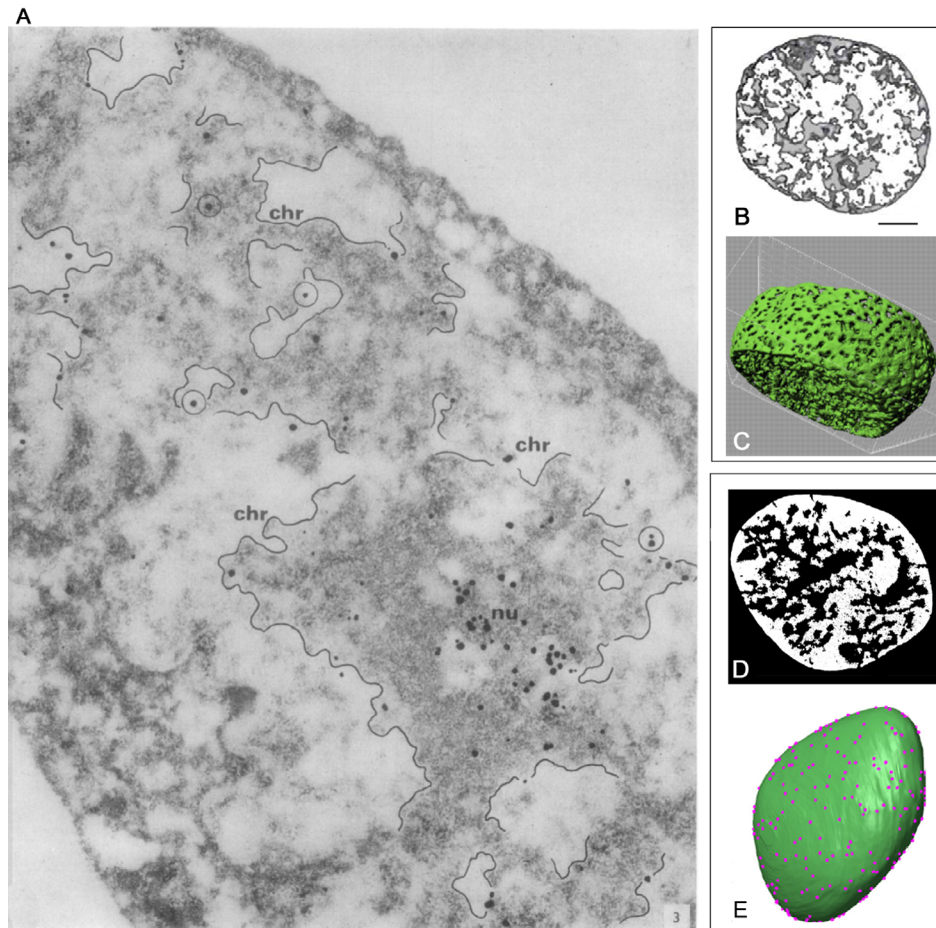


**Figure 3.** Evidence for the interchromatin compartment and perichromatin region based on transmission and scanning EM. A) EM auto radiography of a monkey kidney cell nucleus by Fakan and Bernhard in 1971 provides the first evidence for a non-random nuclear topography of transcription in a mammalian cell nucleus. Reproduced with permission.<sup>[80]</sup> Copyright 1971, Elsevier. The image shows an ultrathin section of a monkey kidney cell nucleus with a nucleolus (nu) and extranucleolar region. The cell was fixed after applying a 5 min pulse-labeling with 3H-Uridine. EM autoradiography shows silver grains, indicating the incorporation of 3H-Uridine into newly synthesized RNA. Some silver grains are surrounded by a circle with a radius of 120 Å indicating the resolution of this technique. Regressive EDTA staining of DNA resulted in very weakly stained, bleached chromatin clusters in contrast to the comparatively intense staining of RNPs within the interchromatin space. Borders are marked with added lines. Silver grains are strongly enriched in the border zone between EDTA-resistant RNP structures and the bleached chromatin.” In subsequent studies the border zone was further defined as the perichromatin region (PR) lining the IC channels (for further details, see text). B) Top view on a 250 nm thick median, nuclear section obtained with 3D block face-scanning electron microscopy of a hepatocyte nucleus shows chromatin clusters (gray pervaded by an extended interchromatin space (white) Adapted with permission.<sup>[89]</sup> Copyright 2009, Springer Nature. This section was reconstructed from five sequential images. Each new image was recorded after slicing away another 50 nm thick section. C) Side view on a more extended 3D reconstruction of BF-SEM images from the same nucleus shows little holes that reflect interchromatin channels pervading the layer of heterochromatin beneath the nuclear envelope (not recorded) Adapted with permission.<sup>[89]</sup> Copyright 2009, Springer Nature. D) Image of a mouse retina nucleus studied with FIB-SEM confirms chromatin clusters pervaded by an interchromatin space with channels extending through a thick peripheral chromatin layer. Reproduced with permission.<sup>[90]</sup> Copyright 2017, Elsevier. E) 3D reconstruction of the same nucleus shows the exit sites (red) of peripheral IC channels as proxies for NPC locations. Scale bar: 2 μm.

nuclear topography of nucleic acids from similar appearing and abundant proteinaceous structures without a need for additional staining protocols. Using this method, Strickfaden and colleagues studied nuclei from various cell types and species, including human HeLa cells, established from a cervical cancer (Figure 4A,B).<sup>[92]</sup> These ESI images show short granular chromatin chains with diameters between 12.6 and 21.6 nm embedded in a DNA-free space with protein rich interchromatin fibrils (note the striking similarities with ChromEMT images from U2OS cell nuclei in Figure 4B). A comparison of nuclear architectures between cell lines that strongly differ in

their functional states revealed marked differences with respect to the distribution of chromatin between the INC and ANC, the density of chromatin networks and diameters of chromatin chains, as well as the width of IC channels (compare 4.2 below).<sup>[92]</sup> In agreement with such structural differences, the transcriptomes of cancer cell lines, such as HeLa, and normal tissue cells differ greatly although causal connections have remained elusive. An RNA sequencing study of a HeLa cell line revealed 1907 genes (of which 805 are protein coding) that were more highly expressed in HeLa than in any tissue in the BodyMap.<sup>[93]</sup>

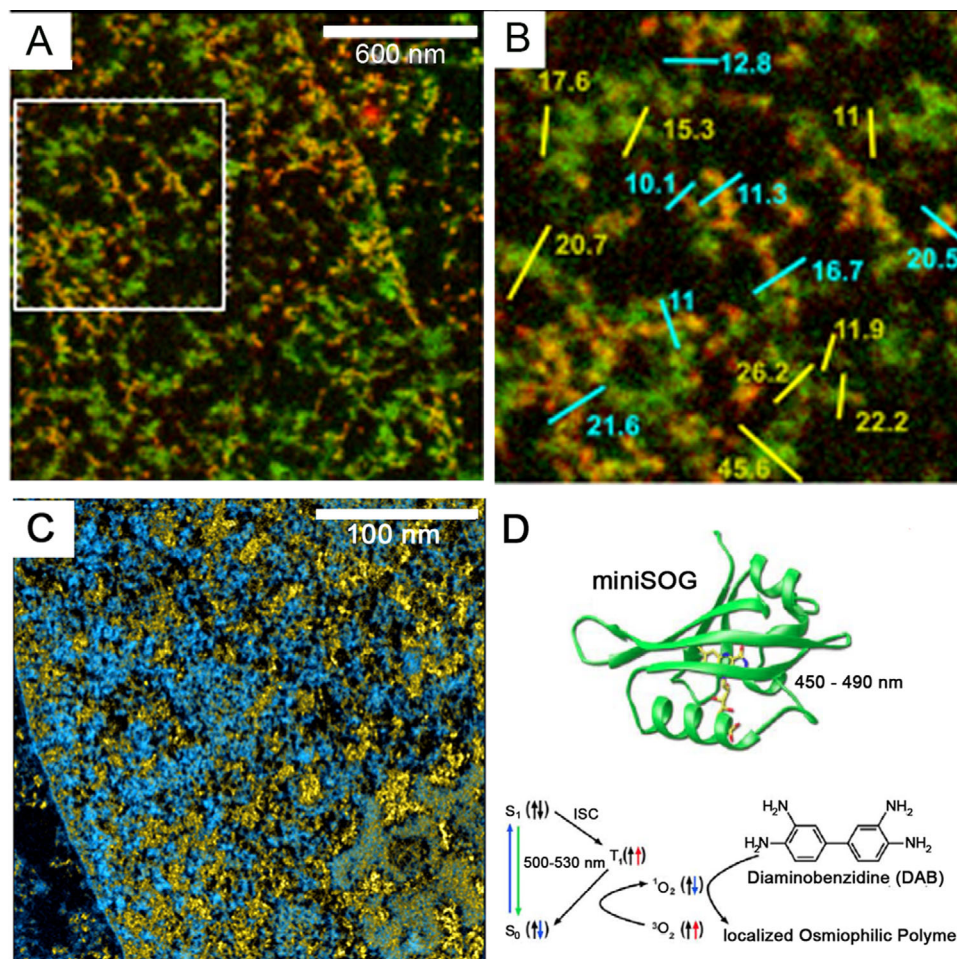


**Figure 4.** Electron spectroscopic imaging (ESI) of chromatin clusters and interchromatin channels enriched with the DNA repair protein p53BP1. A) ESI micrograph of a 50 nm ultrathin section from a HeLa cell nucleus. Nucleic acids were identified due to their high content of phosphorous atoms (red channel) and proteinaceous interchromatin fibrils by their content of nitrogen atoms (green channel) Scale bar: 600 nm. B) Enlarged view of the box framed in (A). Diameters between 12.6 and 21.6 nm were measured for chromatin fibers (cyan lines) and between 11 and 45.6 nm for interchromatin fibrils (yellow lines). Reproduced with permission under the terms of the CC-BY-ND 4.0 International license.<sup>[92]</sup> Copyright 2019, the Authors. Published by bioRxiv. C) ESI micrograph of a 50 nm ultrathin nuclear section from a U2OS cell (Strickfaden and Hendzel unpublished results). U2OS cells overexpressed the DNA repair protein p53BP1 tagged with miniSOG. Overexpressed p53BP1 (false colored in blue) is detected in interchromatin channels and lacunas, pervading between chromatin domain clusters (CDCs) (yellow). Scale bar: 100 nm. D) 3D structure of miniSOG (top) and scheme of the staining procedure of miniSOG tagged proteins (bottom). Reproduced with permission.<sup>[94]</sup> Copyright 2011, PLoS One.

Figure 4C shows a 50 nm ultrathin section of a U2OS cell nucleus recorded with ESI that demonstrates the enrichment of an overexpressed 53BP1 tagged with miniSOG (Figure 4D) within the IC channel system and exclusion from compact chromatin.

53BP1 plays a role in non-homologous end joining (NHEJ) repair and forms aggregates with other proteins.<sup>[95]</sup> In line with the IC hypothesis and limited accessibility hypothesis described in Section 2, we argue that NHEJ and other mechanisms of DNA repair are carried out within the ANC. An electron microscopic investigation of nucleotide excision repair (NER) in human cell lines has shown that following UV-irradiation, XPA and XPC, two proteins involved in the chromatin associated NER complex, accumulate within the PR.<sup>[39]</sup> To enable the execution of DNA repair within the ANC, we postulate that repair of DNA damage caused within the INC requires movements of damaged DNA into the ANC. Notably, 53BP1 binds to the repressive histone modifications H4K20m3 and H3K9m3 suggesting the ability of

53BP1 to diffuse into compact CDs in the INC and possibly trigger the relocation of damaged DNA from the INC into the ANC prior to the execution of repair.<sup>[95]</sup> The repair of damaged DNA molecules alone, however, may not suffice to restore the functional integrity of the genome, but requires the restoration of the structural and functional nuclear landscape present before the DNA damage occurred. Accordingly, damaged sequences located in compact CDs of the INC, but moved into the ANC for repair, must be relocated into the INC thereafter.

### 3.3. Evidence Obtained with ChromEMT, Soft X-Ray Tomography and Block Face Electron Microscopy of Whole Vitreously Frozen Cells

ChromEMT is based on a combination of electron microscopy tomography (EMT) with a protocol that selectivity enhances the



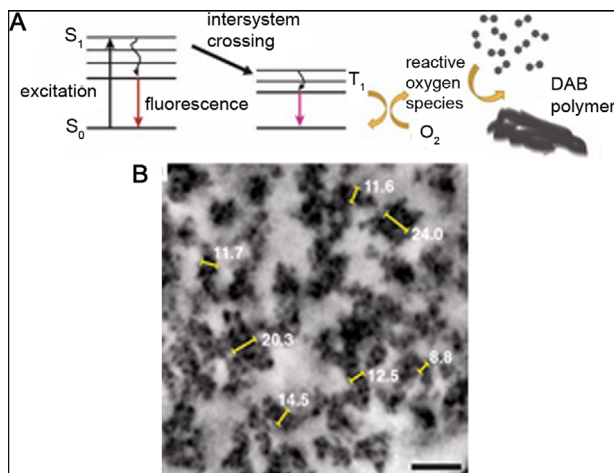


**Figure 5.** Chromatin clusters and interchromatin channels studied with ChromEMT. A) The scheme depicts the generation of diaminobenzidine (DAB) polymers used for the selective enhancement of DNA contrast in ChromEMT. B) Assemblies of nucleosomes (NCs) revealed with ChromEMT show diameters between 5 and 24 nm, with different particle arrangements, densities, and structural conformations. A DNA free interchromatin space extends between these nucleosome assemblies, which we consider as the finest channels of the IC. Scale bar: 50 nm. Reproduced with permission.<sup>[96]</sup> Copyright 2017, American Association for the Advancement of Science (AAAS).

contrast of DNA. Using this method, Ou and colleagues studied nuclei of primary human small airway epithelial cells (SAECs) and demonstrated assemblies of nucleosomes in granular chains with diameters between 5 and 24 nm (Figure 5A,B).<sup>[96]</sup> Such granular chains are likely derived from nucleosome clusters (NCs).<sup>[97]</sup> Apparently, particle arrangements, densities, and structural conformations of the chains differ. It is not clear yet, whether this variability argues for disordered structures (presenting a random walk nucleosome chain) or reflects records of ordered structures, capable of dynamic changes with functional demands.<sup>[98]</sup>

Using soft X-ray tomography (SXT) combined with 3D X-ray reconstructions, Le Gros et al. followed the differentiation of nuclei from stem cells into neuronal progenitors and mature olfactory sensory neurons.<sup>[99]</sup> Interconnected networks of euchromatic and heterochromatic compartments with distinct borders persisted throughout differentiation, but their spatial arrangements and chromatin compaction changed profoundly. SXT like ESI does not require any additional staining protocol. Despite an ultrastructural resolution of SXT down to about 25–50 nm,<sup>[100]</sup> the 3D reconstructions of nuclei shown by the authors do not depict the IC channel networks detected in other EM studies (Figures 3 and 4) and by super-resolved fluorescence microscopy (Section 4). This apparent discrepancy may be explained as a consequence of the evaluation procedure. Le Gros and colleagues measured for each voxel a linear absorption coefficient for carbon, relying on the assumption that a higher carbon concentration distinguishes heterochromatin from euchromatin. Based on LAC measurements, all voxels in computer-generated SXT orthoslices were arbitrarily classified and color-coded as either euchromatin or heterochromatin.

Recently, a platform for 3D correlative super-resolution fluorescence microscopy and FIB-milled block-face EM across entire

vitro frozen cells was developed.<sup>[101]</sup> This method preserves native ultrastructure, but despite the potential of this approach to detect protein–ultrastructure relationships, it does not contribute to the validation or rejection of the interchromatin compartment as a major feature of the nuclear landscape. For this purpose, it is necessary to distinguish the topography of DNA and various RNAs. Combining serial block face scanning electron microscopy with a cytochemical reaction for the selective staining of DNA, Fakan and co-workers were able to demonstrate clearly the crumpled nature of the chromatin pervaded by the interchromatin compartment (Figure 3B,C).<sup>[89]</sup>

## 4. Support of the ANC-INC Model with Super-Resolved Fluorescence Microscopy

### 4.1. A Range of Super-Resolved Microscopic Approaches has Become Available

Super-resolved fluorescence microscopy has overcome the classical limit of light microscopic resolution with a lateral resolution of about 200 nm (Abbe limit) and an axial resolution of about 600 nm (for reviews, see refs. [102–105]). Widely used methods include stimulated emission depletion (STED) microscopy,<sup>[106,107]</sup> structured illumination microscopy (SIM)<sup>[108,109]</sup> (for review, see ref. [110]). 3D SIM provides a lateral resolution of  $\approx 100$  nm and an axial resolution of  $\approx 300$  nm. This twofold gain in linear resolution compared with the resolution of a typical confocal laser scanning microscope appears modest but is equivalent to an  $\approx$ eightfold volumetric improvement.<sup>[102,105]</sup> SIM allows multicolor studies of cell samples prepared for standard fluorescence microscopy and does not require special fluorophores apart from the need that they should be reasonably resistant to photobleaching.<sup>[102]</sup>

A further increase of resolution has become possible with various approaches of single molecule localization microscopy (SMLM) known as PALM, STORM, etc.<sup>[111–113]</sup> These approaches are based on the principle that single fluorescence point sources, such as small DNA segments hybridized with fluorescent DNA probes<sup>[114]</sup> or “blinking” quantum dots, that is, dots, which emit a burst of photons<sup>[111]</sup> or even individual “blinking” fluorophores<sup>[115]</sup> can be recorded and localized with a much better precision than the resolution limit of the microscope. Accordingly, an approach termed spectral precision distance microscopy allows to determine precisely the distance between two differentially colored fluorescence point sources, even when they are positioned closer to each other than the resolution limit of the recording microscope.<sup>[114]</sup> Both sources yield a single fluorescent signal in case that they emit fluorescent light with the same wavelength. The possibility to record the precise position of very large numbers of independent blinking events in space from fluorophores conjugated to a cellular target of interest has opened the way to super-resolved localization microscopy with PALM<sup>[112]</sup> and STORM.<sup>[113]</sup> Further improvements paved the way to use fluorophores conventionally used in microscopic studies of the cell nucleus.<sup>[116–118]</sup> The highest light optical resolution in the analysis of nuclear genome nanostructures has been obtained so far with SMLM and is currently in the order of 20–50 nm and even better in special circumstances.<sup>[119]</sup> The different methods

of super-resolved microscopy which can be employed for studies of the nuclear organization have different advantages and limitations. Resolution is only one of many parameters, which need to be considered. What matters is not always the highest resolution, but the right resolution needed to solve a given biological problem. Other parameters are of equal importance, such as structure integrity of the sample, the choice of fluorophores, optimally suited for the labeling of chosen targets with little fluorophore bleaching, optimal signal, and noise levels recorded by detectors with high quantum efficiency, software for image analysis and 3D reconstructions.<sup>[120]</sup>

#### 4.2. Nuclear Landscapes of Cell Types are Shaped by a Wide Variation of IC Channels and Lacunas

Principle features of the ANC-INC model were consistently observed in all studied cell types from various mammalian species. Numerous 3D SIM studies combined with quantitative 3D image analyses revealed CDs, CDCs and CTs, the IC and the PR (compare Figure 1). Readers are referred to the respective literature and recent reviews.<sup>[31,35,46,47,74,102,121–125]</sup> Profound differences, however, were noted in different cell types both with regard to the width of IC channels and lacunas and the quantity and distribution of chromatin assigned to the ANC or INC. Such differences are exemplified for human hematopoietic cell differentiation (Figure 6A)<sup>[123]</sup> and for preimplantation development of in vitro fertilized (IVF) bovine embryos (Figure 6B1–B6).<sup>[35]</sup> Voxels of serial SIM sections recorded from individual, DAPI-stained nuclei were assigned to seven DAPI intensity classes as proxies for differences of chromatin compaction.<sup>[126]</sup> In preimplantation, nuclei of cells close to the time of major genome activation at the 8-cell stage, we noted a large central IC lacuna which occupied a major part of the nuclear (Figure 6B3). Changes observed in bovine IVF preimplantation embryos were mimicked by similar changes in cloned preimplantation embryos (Figure 6B7–B12). The size of cell nuclei decreased during preimplantation development and central IC lacuna disappeared in line with a reorganization of the chromatin landscape, where CTs contact each other to an extent that they cannot be distinguished from each other as distinct entities without a differential coloring by chromosome painting, a situation typical for most somatic cell types. Consider, for example, the bovine fibroblast nucleus shown in Figure 6C13–C15. In contrast, certain interphase nuclei observed during preimplantation development of IVF and cloned bovine embryos provide examples, where some CTs at face value appear fully separated from neighboring CTs by wide IC channels (Figures 6B3 and 9; Figure 6C16–C19). Notably, the profound changes of nuclear architecture observed during bovine preimplantation development is dominated by a change of the IC pattern. For example, Figure 8B6,B12 shows a similar context of chromatin domain clusters (CDCs) pervaded by IC channels, but represent enlargements of boxed areas from nuclei with drastically different global landscapes presented in Figures 6B5 and 9, respectively.

The highly dynamic nature of higher-order chromatin organization upon transient stress was demonstrated in a SMLM study of cultured mouse cardiomyocytes.<sup>[75]</sup> This study revealed a very pronounced increase of chromatin compaction, when cardiomy-

ocytes were kept under oxygen and nutrient deprivation. Under such conditions, a strong increase of chromatin compaction was observed together with widening of the IC and a reduction of transcription. In both control and deprived nuclei, H3K14ac, a histone mark associated with transcriptionally permissive chromatin, was enriched in chromatin lining the IC, but the number of immunodetectable H3K14ac-sites was strongly decreased during oxygen and nutrient deprivation. These structural and functional effects were reversible upon restitution of normoxia and nutrients. Restoration of an open chromatin structure upon recovery even provoked a transiently more open chromatin structure and a transitory increase in transcription.

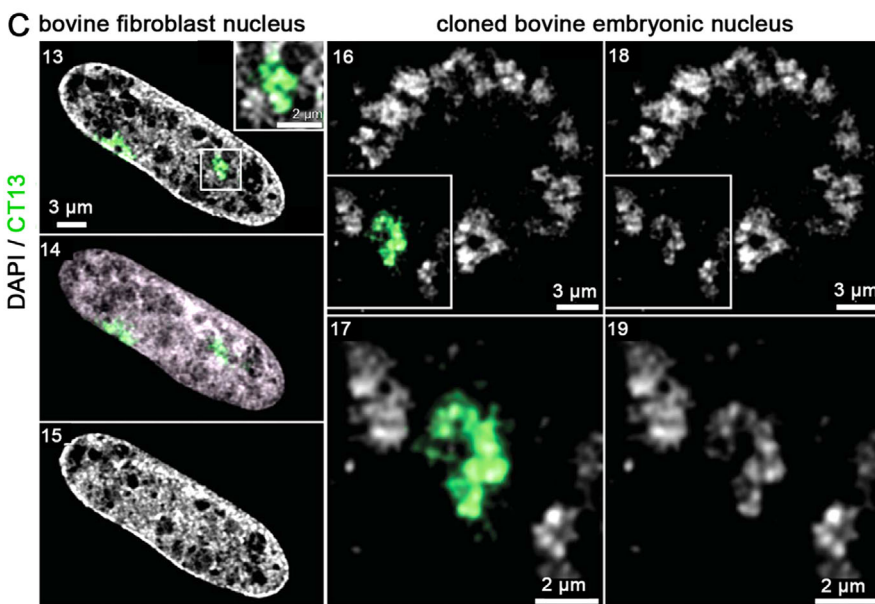
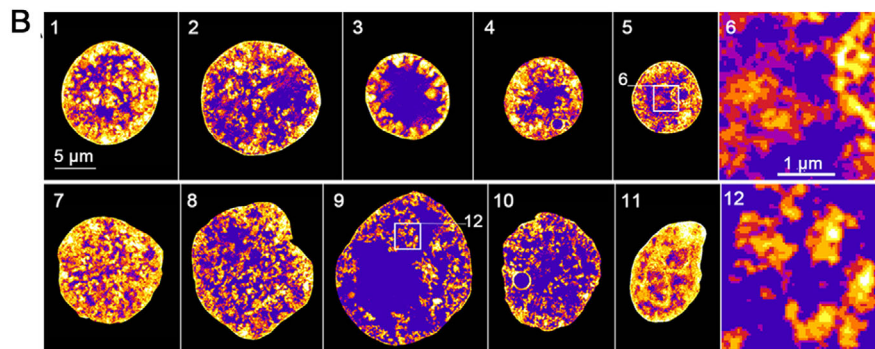
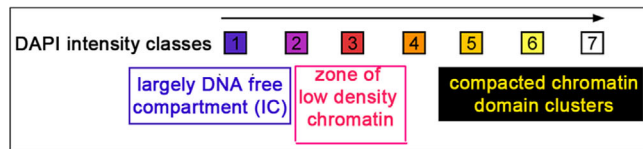
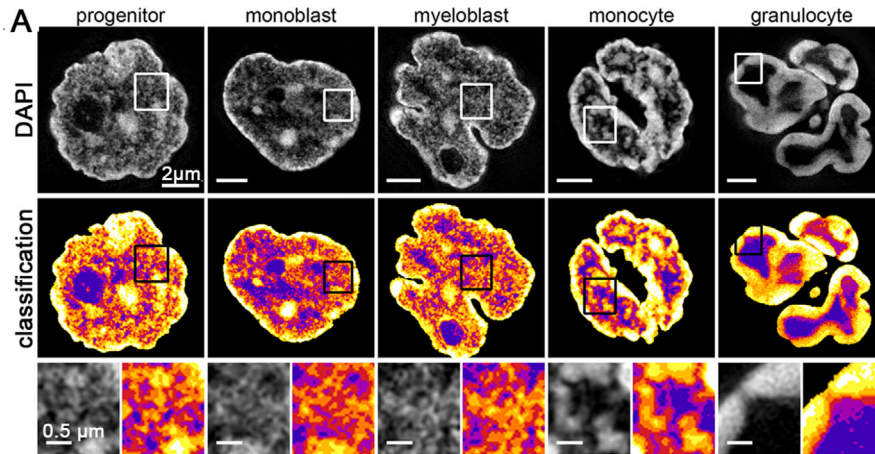
#### 4.3. Quantitative Assignment of Functional Markers to 3D Chromatin Compaction Maps Representing the ANC and INC

3D color heat maps based on DAPI intensity classes shown in Figure 6 were used as proxies for a quantitative 3D assignment of functionally important markers (Figure 7; compare Figure 1).<sup>[74,126]</sup>

Figure 7A illustrates the topographical context of the seven DAPI intensity classes in a single SIM section of a DAPI-stained human fibroblast nucleus. The lowest DNA density class 1 represents the IC with splicing speckles and nuclear bodies.<sup>[35,123,124]</sup> Intensity classes 2 and 3 represent the less-compacted chromatin of the PR, which lines the IC and shows a significant enrichment for RNAPII, and epigenetic markers indicating transcriptionally competent chromatin.<sup>[35,74,123–125]</sup> In line with these assignments, RNA synthesis is most prominent within the PR.<sup>[121,125]</sup> Moreover, active regulatory sequences were found enriched within the PR while inactive sequences were found enriched toward the compacted interior core of CDCs.<sup>[46,47]</sup> Class 4 apparently depicts a transition zone between the two co-aligned active and inactive nuclear compartments (ANC and INC). Intensity classes 5–7 represent more compacted chromatin in the interior of CDCs enriched with epigenetic markers for transcriptionally repressed heterochromatin.<sup>[35,74,123,124]</sup> Assignments of markers for active and repressed chromatin to adjacent DAPI intensity classes can somewhat vary in different cell types and also within a given cell type depending on variations of experimental conditions. It should be emphasized here that various parts of the IC in such a colored section appear like isolated blue holes of various sizes and with multiform edges. 3D reconstructions, however, prove the formation of an interconnected network of IC channels (3D movies in,<sup>[46,74]</sup> preferentially lined by chromatin with epigenetic marks for transcriptionally competent chromatin. Notably, these principal structural features of the ANC-INC model are also maintained in cohesin depleted nuclei<sup>[124,125]</sup> and even reconstituted in these cells after mitosis.<sup>[124]</sup>

#### 4.4. IC Channels are Enriched with Transcribed RNAs and Connected to Nuclear Pores

3D FISH of human fibroblasts with a cDNA probe, enriched in genome wide sequences from transcribed genes (Figure 8A1–A3), revealed an enrichment of RNA sequences within IC channels (Figure 8A3). Most hybridized sequences were likely present



as RNPs. This FISH experiment was performed under denaturing conditions, suggesting an enrichment of the transcribed genes in chromatin lining IC channels. IC channels penetrate the layer of heterochromatin beneath the nuclear envelope and are directly connected to NPCs (Figure 8B–D).

The nuclear envelope may appear as a smooth-surfaced outer boundary but in many cell types, including cancer cells, invaginations reach deep inside and can even traverse the entire nucleus.<sup>[127]</sup> Such envelope invaginations allow for close topographical relationships between NPCs and chromatin, as well as nucleoli, apparently located in the nuclear interior. In conclusion, we argue that NPCs and the IC should be considered as an integrated functional system—to accomplish the needs of nuclear import/export functions even for chromatin embedded deep in the nuclear interior. Nuclear invaginations covered with NPCs may serve as a back-up system in case of extraordinary import/export demands.<sup>[128]</sup> Nuclear envelope invaginations allow for close topographical relationships between NPCs and chromatin, as well as nucleoli, apparently located in the nuclear interior.<sup>[127,128]</sup>

On their way through the peripheral layer of heterochromatin associated with the lamina toward NPCs, IC channels apparently extend between lamina-associated domains (LADs).<sup>[129,130]</sup> The lamina below the nuclear envelope is composed of nuclear lamins. Lamins are also found in the interior of the nucleus. Molecular studies and advanced imaging approaches, including live-cell studies, have demonstrated that lamin A is responsible for the global long-range stability of chromatin throughout the whole nuclear space, whereas other structural proteins, such as BAF, Emerin, lamin B, CTCF, and cohesion mildly affect the type of the diffusion, while the extent of motions is not affected.<sup>[131]</sup> A-type lamins or a protein complex containing lamin A may generate scaffolds expanding through the nuclear space that regulate many functions, including chromatin organization, gene transcription, DNA replication, DNA damage response, as well as cell cycle progression, cell differentiation, and cell migration.<sup>[131]</sup> The scaffolding protein SAF-A interacts with chromatin-associated RNAs and forms a chromatin mesh in a transcription-dependent manner.<sup>[132]</sup> Though current evidence favors the perspective that folded chromatin per se forms a structural milieu for nuclear functions,<sup>[133]</sup> scaffolding structures with

a multifaceted biochemical composition and structural organization formed within the ANC may also essentially contribute to shaping the functional nuclear architecture.<sup>[5,132,134]</sup> Some scaffolding structures, including A-type lamins may start at NPCs and expand into the nuclear interior along the preformed routes of the IC channel system, while others are generated in the nuclear interior.<sup>[135]</sup> To what extent such scaffolding structures might contribute to mechanical cues modulating gene expression is an open question.<sup>[136]</sup>

## 5. A Match between the ANC-INC Model and the Liquid Droplet Model of Higher Chromatin Organization

Our current conceptual understanding of higher-order chromatin organization has been strongly influenced by models derived from polymer physics. Polymer models of chromatin organization assume that chromatin fibers are composed of a large number of “elementary units” (nucleosomes plus linkers) with specific differences in the DNA sequence and a variety of DNA and histone modifications. Complex interactions take place within and between these fibers.<sup>[137–139]</sup> Though *in vitro* assays with diluted chromatin readily demonstrate 30 nm thick chromatin fibers, such fibers were only exceptionally observed in EM studies of cell nuclei.<sup>[140,141]</sup> Evidence provided by Maeshima and colleagues indicates that the interior of CDs is densely packaged to an extent that nucleosome interactions between neighboring  $\approx 10$  nm thick chromatin fibers prevent the formation of 30 nm thick fibers (Figure 9A).<sup>[142,143]</sup>

According to the Maeshima model, the dense packaging of irregularly folded 10 nm fibers results in a liquid-like behavior of the chromatin domain structure. The diffusion of individual macromolecules into the interior of compact CDs is possible, yet highly constrained, whereas large transcription complexes are excluded (Figure 9B,C). Monte Carlo simulations suggest that constrained diffusion of individual macromolecules into the interior of CDs with nucleosome concentrations of about 0.3–0.5 mM (corresponding to 40–60 Mb  $\mu\text{m}^{-3}$ ) is possible, whereas such densities result in an accessibility barrier for molecular complexes with diameters  $> 20$ –25 nm.<sup>[45]</sup> For comparison, the size of

**Figure 6.** Both the interchromatin compartment and chromatin arrangements undergo major changes during human hematopoietic cell differentiation and bovine preimplantation development. A) Representative nuclei of cycling and terminally differentiated human hematopoietic cell types. Reproduced with permission.<sup>[123]</sup> Copyright 2015, Springer Nature. Upper row: SIM midsections of DAPI-stained nuclei with examples of human hematopoietic precursor cells (progenitor cells, monoblasts, and myeloblasts) and terminally differentiated cells (monocytes and granulocytes). Note obvious differences with regard to nuclear shapes and extent of nuclear envelope invaginations. Middle row: The same nuclear midsections shown with color-coded DNA density classification (classes 1–7). Bottom row: Enlargements of framed boxes in the middle row (for further details, see ref. [123]). Scale bars: 2  $\mu\text{m}$ ; 0.5  $\mu\text{m}$  for the enlarged insets. A, below) Schematic draft for a color coded DNA density classification used as a proxy for increasing chromatin densities: Class 1 (blue) background intensity represents the IC; classes 2 and 3 represent the PR, class 4 is considered a transition zone, classes 5–7 comprise the compact chromatin domains of the INC,<sup>[126]</sup> compare also Figure 7. B) Nuclei representative for different stages of *in vitro* fertilized (1–5) and cloned bovine preimplantation embryos (7–11) (for details, see ref. [35]). Nuclei 1–3 and 7–9 exemplify stages prior to and at major genome activation (MGA), which was demonstrated to occur at the 8-cell stage of IVF embryos: Nuclei 4, 5 and 10, 11, respectively, represent stages after MGA. Chromatin arrangements, as well as the arrangements of the IC (blue), undergo major changes during preimplantation development. After MGA nuclear volumes decreased significantly in both IVF and cloned embryos (for quantitative measurements, see ref. [35]). Despite these major changes of nuclear organization, boxed areas (6, 12) from 5 and 9 show chromatin domain clusters pervaded by the IC. Reproduced with permission.<sup>[35]</sup> Copyright 2014, Taylor & Francis. C) Panels 13–19 further demonstrate a major impact of cloning on nuclear shape and size, as well as on the spatial organization of chromosome territories and the IC. (13) shows a mid-plane and (14) a top nuclear section with two painted BTA 13 territories recorded with a laser confocal scanning microscope from an ellipsoidal-shaped, DAPI-stained (false-colored gray) bovine fetal fibroblast nucleus. Territory borders can only be discriminated after CT painting (15). In contrast, a complete separation of these painted CTs from neighboring CTs was noted in nuclei of IVF embryos close to MGA (not shown), as well as in nuclei of cloned preimplantation embryos at a similar stage of preimplantation development (16–19). Scale bars: 3  $\mu\text{m}$ ; insets: 2  $\mu\text{m}$ .

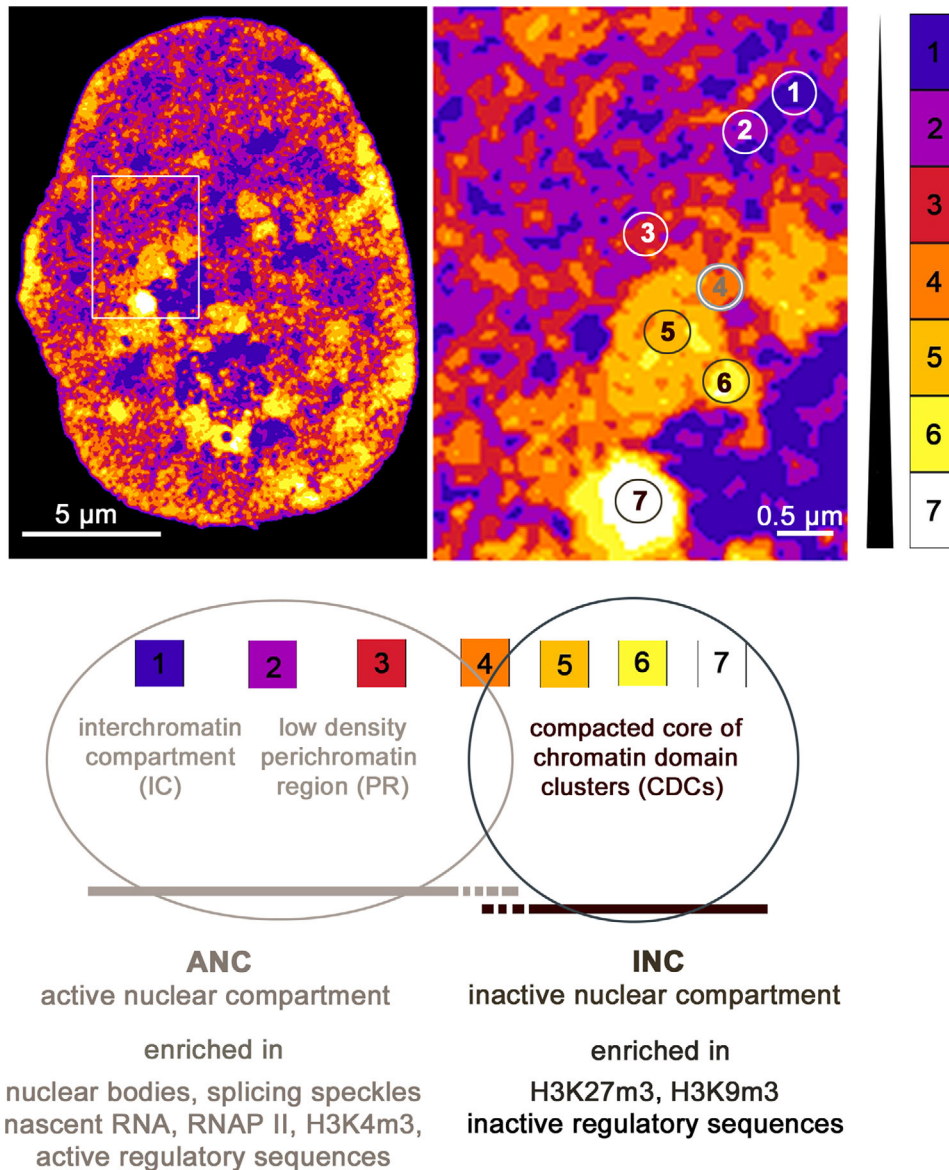


**Figure 7.** ANC-INC model: Synopsis of relationships between chromatin compaction and the enrichment of functional markers representative for the active or inactive nuclear compartment. See Figures 1 and 6 and refs. [35,46,74,121,123,125,126] for details.

individual transcription factories was estimated to be between 35 and 75 nm using both EM and super-resolution microscopy.<sup>[145]</sup> Other macromolecular complexes, for example, replication complexes may even be larger.<sup>[146]</sup> Furthermore, the Maeshima group described the formation of a loose spatial genome chromatin network via RNAPII-Ser5P, which can globally constrain chromatin dynamics.<sup>[147]</sup> Accessibility measurements using image correlation spectroscopy suggested a substantial accessibility barrier for particles as small as 10–20 nm into chromatin domains with DNA densities on the order of about 1 mM.<sup>[148,149]</sup> It was argued that phase-separated droplets of distinct chromatin states within the nucleus are mediated by class-specific interactions of multivalent proteins, such as H3K27m3, H3K9m3, HP1 $\alpha$ , and polycomb group proteins.<sup>[150–152]</sup> In addition, phase separation may also help to concentrate certain molecules and exclude

others creating diffusion barriers in the crowded environment of the IC.<sup>[153,154]</sup> (Figure 2D)

## 6. Concluding Remarks and Future Perspectives

In this article, we have described current evidence for three interconnected hypotheses of the ANC-INC model—the IC hypothesis, the limited accessibility hypothesis and the dynamic interactions hypothesis (Section 2). Although current evidence for these hypotheses is by no means compelling, it seems strong enough to warrant further studies, as well as attempts to integrate this evidence into models of the nuclear architecture supported by other experimental strategies, such as Hi-C,<sup>[155–157]</sup> ChIA-Pet,<sup>[158,159]</sup> and GAM.<sup>[160]</sup> Notably, despite their possibilities

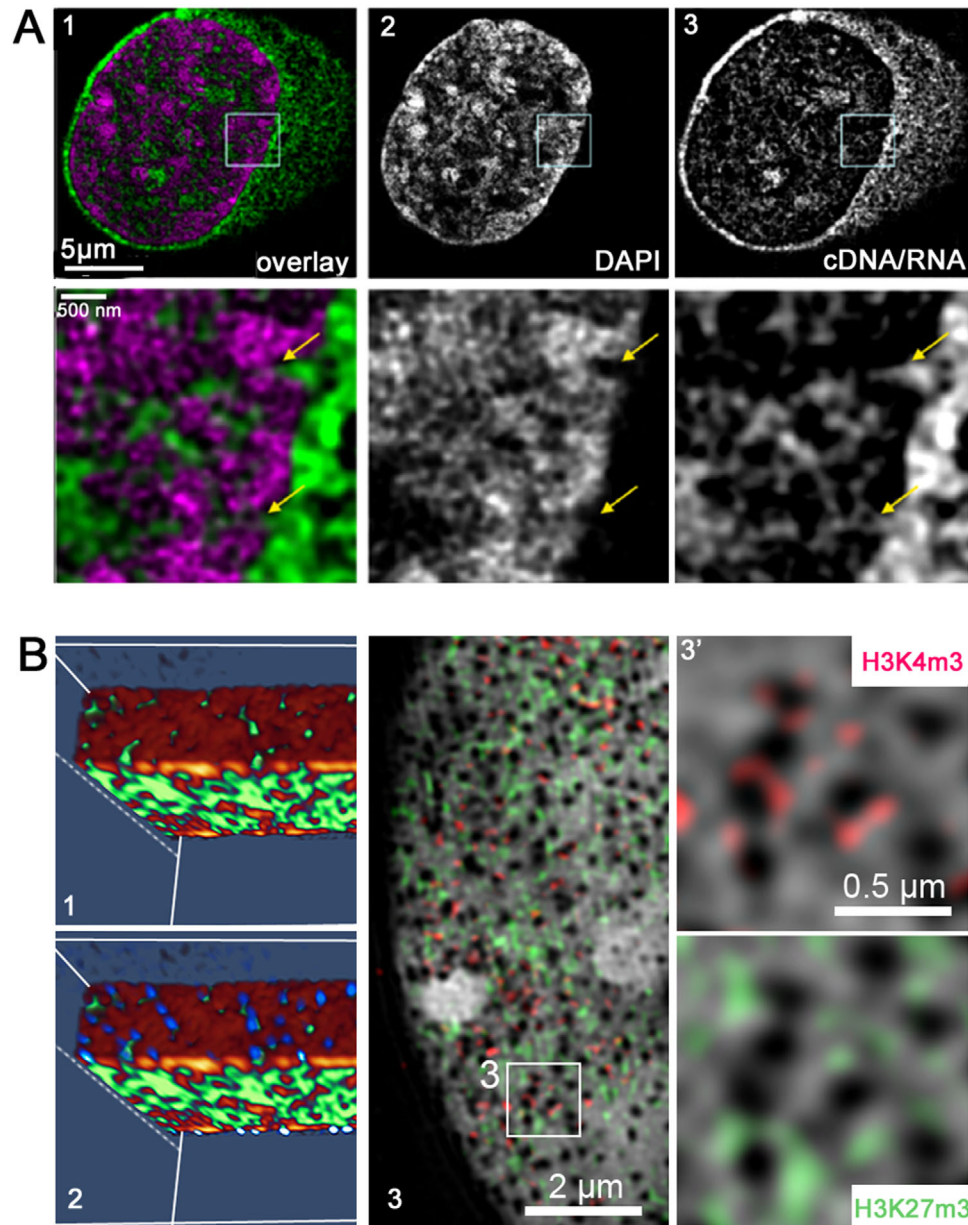


**Figure 8.** 3D structured illumination microscopy (SIM) demonstrates an enrichment of ribonucleic acids in the ANC and direct connections of IC channels with nuclear pores. A) Human fibroblast nucleus recorded with SIM after 3D FISH with a global cDNA probe (Silahtaroglu and Cremer, unpublished results). This probe hybridized to RNA transcribed from numerous genes, as well as to denatured, nuclear DNA targets, which served for RNA transcription. Upper panel: Mid-nuclear sections: 1) Overlay: DAPI: magenta; RNA and DNA targets hybridized with the cDNA probe: green. 2) DAPI only. 3) cDNA/RNA only. Lower panel: respective magnifications of the boxed areas at the border of nuclear mid-sections. As predicted by the ANC-INC model, we find a strong enrichment of the target sites within the IC and the lining chromatin domains. Scale bar: 5  $\mu\text{m}$ , inset magnifications 500 nm. B-1) 3D volume rendering of a cuboidal shaped part of the nuclear periphery with DAPI-stained chromatin colored in brown and the IC in green. Green dots represent IC channels penetrating the peripheral heterochromatin. 2) Same 3D volume rendering shows nuclear pore complex immunostained with an antibody against Nup153 (blue). This result demonstrates that IC channel start/end at nuclear pores. 3) Partial apical SIM section from a mouse myoblast nucleus with transverse cuts through IC channels (black holes) penetrating the layer of heterochromatin beneath the nuclear lamina together with red marked H3K4m3 and green marked H3K27m3 signals. Scale bars: 2  $\mu\text{m}$ . insets: 0.5  $\mu\text{m}$ . Adapted with permission.<sup>[74]</sup> Copyright 2014, Springer Nature.

for genome wide studies, methods based on 3D contact frequencies (Hi-C, ChIA-Pet) or the spatial proximity of DNA sequences (GAM) are not suitable to visualize the interchromatin compartment. Whereas Hi-C-based 3D models of the higher-order chromatin architecture show an interchromatin space between

chromatin loops with open configurations<sup>[11]</sup> or little chromatin balls/droplets,<sup>[61]</sup> we miss any hint on the drastic differences of the IC with respect to its expansion and cell type specific arrangements within the nuclear space (demonstrated in Figure 6). Whereas the existence of CTs has become a generally accepted

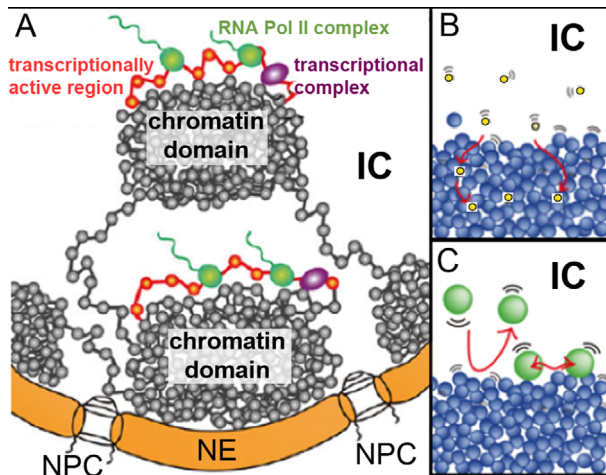


**Figure 9.** Polymer melt model of chromatin domain structure. A) According to the liquid drop model of Maeshima and colleagues, chromatin domains are built up by irregularly folded 10 nm thick chromatin fibers. Active chromatin regions (red) are transcribed on the domain surfaces with transcriptional complexes (purple) and RNA polymerase II (green). Adapted from ref. [144]. B) Constrained diffusion of single transcription factors ( $\varnothing \approx 5$  nm, yellow), into a liquid drop like CD. C) Larger complexes ( $\approx 30$  nm, green) such as mRNP are excluded from liquid drop like CDs. Adapted with permission.<sup>[45]</sup> Copyright 2015, IOP Publishers.

feature of higher-order chromatin organization<sup>[162]</sup> the true 3D and 4D organization of chromatin loops and chromatin domains has remained elusive. This information is indispensable for an understanding of the functional nuclear compartmentalization, in particular for a solution of the problem, whether transcription, chromatin replication, and repair mechanisms occur at the surface of CDs or in the interior or at any site. Recent evidence indicates that nucleosomes form nucleosome clusters with sizes from a few kb DNA upward.<sup>[97]</sup> At the next level, NCs may allow the formation of individual chromatin loop domains in the order of 100–200 kb.<sup>[163,164]</sup> Several loops form chromatin domains<sup>[163]</sup> and several CDs form CDCs, which in turn form CTs.

Integrative biophysical and biochemical research strategies are imperative for a better understanding of the dynamic nuclear architecture and the molecular mechanisms involved in the interplay between nuclear architecture and function,<sup>[165–167]</sup> for review, see ref. [168]. Such strategies will be discussed in a subsequent review with a focus on high-resolution studies of chromatin compaction and accessibility (Cremer et al., in preparation).

Major differences of nuclear phenotypes occur during development of multicellular organisms from the fertilized egg to the formation, maintenance, and senescence of cell types in whole tissues. The extent to which these differences may be causally connected with specified, functional tasks, defines a major issue for future 4D nucleome research. As a caveat, we emphasize that the description of structural components and compartments of cell nuclei in studies from us and others are still mainly based on 3D microscopic investigations of fixed cells. What is least understood at present is the dynamic nature of nuclear structure and function, which implies a preferred location of chromatin loops and chromatin domains or even entire CTs for the proper execution of functional tasks, including a variable course of channels depending on functional needs. To solve

these problems, it will be mandatory to observe movements of DNA sequences and entire CDs between the ANC and INC directly in live cell studies.<sup>[68,73,169–172]</sup>

During recent years, an ever-increasing number of distinguishable cell types were detected in multicellular species. An interdisciplinary community of scientists has started a collaboration to build a human cell atlas. This atlas should define “all human cell types in terms of distinctive molecular profiles (e.g., gene expression) and connect this information with classical cellular descriptions (e.g., location and morphology).”<sup>[173]</sup> The final goal would be “to describe and define the cellular basis of health and disease” (<https://www.humancellatlas.org/>). This project is an enormous endeavor and differs from the Human Genome Project in important ways “owing to unique aspects of cell biology, which requires a distinct experimental toolbox, and includes choices concerning molecular and cellular descriptors.”<sup>[173–176]</sup> In addition, “histological and anatomical information (e.g., cell location, morphology, or tissue context), temporal information (e.g., the age of the individual or time since an exposure), and disease status” must be included, because “such information is essential for harmonizing results based on molecular profiles with rich knowledge about cell biology, histology and function.”<sup>[173]</sup> It is an obvious challenge to combine the human cell atlas initiative with 4D nucleome research to pursue the grand vision “of gaining deeper mechanistic insights into how the nucleus is organized and functions” and “to determine how genome structure and chromatin conformation modulate genome function in health and disease.”<sup>[11]</sup> Evolutionary studies are required to shed more light on the origin of eukaryotes, as well as the emergence and general or restricted availability of mechanisms necessary to drive the structure–function relationships of nuclear organization.<sup>[30,31]</sup>

## Acknowledgements

The authors are grateful to their colleagues Giacomo Cavalli, Job Dekker, Thoru Pederson, and Denise Sheer for helpful discussions and comments on previous versions of this article. The responsibility for all remaining weaknesses lies with the authors. T.C., M.C., and C.C. were supported by grants from the Deutsche Forschungsgemeinschaft (DFG) and the European Community, H.S. by grants from the Canadian Cancer Society Research Institute and the Canadian Institutes of Health Research to M.H. The authors also acknowledge technical support of the Center for Advanced Light Microscopy (CALM) at the LMU Biocenter.

## Conflict of Interest

The authors declare no conflict of interest.

## Keywords

active nuclear compartment (ANC), chromatin domain (cluster) (CDC), chromosome territory (CT), inactive nuclear compartment (INC), inter-chromatin compartment (IC), nucleosome cluster (NC), perichromatin region (PR)

Received: July 31, 2019  
Revised: November 24, 2019

- [1] S. T. Kosak, M. Groudine, *Genes Dev.* **2004**, *18*, 1371.
- [2] T. Misteli, *Cell* **2007**, *128*, 787.
- [3] W. A. Bickmore, B. van Steensel, *Cell* **2013**, *152*, 1270.
- [4] J. Fraser, I. Williamson, W. A. Bickmore, J. Dostie, *Microbiol. Mol. Biol. Rev.* **2015**, *79*, 347.
- [5] A. J. Fritz, N. Sehgal, A. Pliss, J. Xu, R. Berezney, *Genes, Chromosomes Cancer* **2019**, *58*, 407.
- [6] A. Krumm, Z. Duan, *Semin. Cell Dev. Biol.* **2019**, *90*, 62.
- [7] B. van Steensel, E. E. M. Furlong, *Nat. Rev. Mol. Cell Biol.* **2019**, *20*, 327.
- [8] M. W. Vermunt, D. Zhang, G. A. Blobel, *J. Cell Biol.* **2019**, *218*, 12.
- [9] S. Tashiro, C. Lanctot, *Nucleus* **2015**, *6*, 89.
- [10] T. Ried, I. Rajapakse, *Methods* **2017**, *123*, 1.
- [11] J. Dekker, A. S. Belmont, M. Guttman, V. O. Leshyk, J. T. Lis, S. Lomvardas, L. A. Mirny, C. C. O'Shea, P. J. Park, B. Ren, J. C. R. Politz, J. Shendure, S. Zhong, D. N. Network, *Nature* **2017**, *549*, 219.
- [12] C. Rabl, *Morphologisches Jahrbuch* **1885**, *10*, 214.
- [13] T. Cremer, *Von der Zellenlehre zur Chromosomentheorie, Naturwissenschaftliche Erkenntnis und Theorienwechsel in der frühen Zell- und Vererbungsforschung*, Springer, Heidelberg, Germany **1985**.
- [14] T. Cremer, C. Cremer, *Eur. J. Histochem.* **2006**, *50*, 161.
- [15] M. L. Pardue, J. G. Gall, *Proc. Natl. Acad. Sci. USA* **1969**, *64*, 600.
- [16] T. Cremer, C. Cremer, *Eur. J. Histochem.* **2006**, *50*, 223.
- [17] T. Cremer, C. Cremer, P. Lichter, *Human Genetics* **2014**, *133*, 403.
- [18] D. E. Comings, *Am. J. Hum. Genet.* **1968**, *20*, 440.
- [19] F. Vogel, T. M. Schroeder, *Humangenetik* **1974**, *25*, 265.
- [20] K. Scherrer, *Exp. Cell Res.* **2018**, *373*, 1.
- [21] F. H. Crick, *Eur. J. Biochem.* **1978**, *83*, 1.
- [22] F. H. Crick, *Proc. of the Sixth Int. Chromosome Conf., Helsinki* (Eds: A. de la Chapelle, M. Sorsa), **1977**. Elsevier, New York, p. 405.
- [23] I. Solovei, M. Kreysing, C. Lanctot, S. Kosem, L. Peichl, T. Cremer, J. Guck, B. Joffe, *Cell* **2009**, *137*, 356.
- [24] I. Solovei, A. S. Wang, K. Thanisch, C. S. Schmidt, S. Krebs, M. Zwenger, T. V. Cohen, D. Devys, R. Foisner, L. Peichl, H. Herrmann, H. Blum, D. Engelkamp, C. L. Stewart, H. Leonhardt, B. Joffe, *Cell* **2013**, *152*, 584.
- [25] A. L. Olins, D. E. Olins, *Science* **1974**, *183*, 330.
- [26] R. D. Kornberg, *Science* **1974**, *184*, 868.
- [27] K. Luger, A. W. Mader, R. K. Richmond, D. F. Sargent, T. J. Richmond, *Nature* **1997**, *389*, 251.
- [28] G. Felsenfeld, M. Groudine, *Nature* **2003**, *421*, 448.
- [29] N. Gilbert, J. Allan, *Essays Biochem.* **2019**, *63*, 1.
- [30] T. Cremer, M. Cremer, C. Cremer, *Biochemistry* **2018**, *83*, 313.
- [31] T. Cremer, M. Cremer, B. Hubner, H. Strickfaden, D. Smeets, J. Popken, M. Sterr, Y. Markaki, K. Rippe, C. Cremer, *FEBS Lett.* **2015**, *589*, 2931.
- [32] T. Cremer, C. Cremer, *Nat. Rev. Genet.* **2001**, *2*, 292.
- [33] Q. Zhang, K. P. Kota, S. G. Alam, J. A. Nickerson, R. B. Dickinson, T. P. Lele, *J. Cell. Physiol.* **2016**, *231*, 1269.
- [34] J. Kim, K. Y. Han, N. Khanna, T. Ha, A. S. Belmont, *J. Cell Sci.* **2019**, *132*, jcs226563.
- [35] J. Popken, A. Brero, D. Koehler, V. J. Schmid, A. Strauss, A. Wuensch, T. Guengoer, A. Graf, S. Krebs, H. Blum, V. Zakhartchenko, E. Wolf, T. Cremer, *Nucleus* **2014**, *5*, 555.
- [36] P. Bjork, L. Wieslander, *Cell. Mol. Life Sci.* **2017**, *74*, 2875.
- [37] M. J. Hendzel, F. Boisvert, D. P. Bazett-Jones, *Mol. Biol. Cell* **1999**, *10*, 2051.
- [38] S. Fakan, R. van Driel, *Semin. Cell Dev. Biol.* **2007**, *18*, 676.
- [39] L. Solimando, M. S. Luijsterburg, L. Vecchio, W. Vermeulen, R. van Driel, S. Fakan, *J. Cell Sci.* **2009**, *122*, 83.
- [40] J. Rouquette, C. Cremer, T. Cremer, S. Fakan, *Int Rev Cell Mol Biol* **2010**, *282*, 1.
- [41] Y. Chen, Y. Zhang, Y. Wang, L. Zhang, E. K. Brinkman, S. A. Adam, R. Goldman, B. van Steensel, J. Ma, A. S. Belmont, *J. Cell Biol.* **2018**, *217*, 4025.
- [42] I. Masiello, S. Siciliani, M. Biggiogera, *Histochem. Cell Biol.* **2018**, *150*, 227.
- [43] S. A. Quinodoz, N. Ollikainen, B. Tabak, A. Palla, J. M. Schmidt, E. Detmar, M. M. Lai, A. A. Shishkin, P. Bhat, Y. Takei, V. Trinh, E. Aznauryan, P. Russell, C. Cheng, M. Jovanovic, A. Chow, L. Cai, P. McDonel, M. Garber, M. Guttman, *Cell* **2018**, *174*, 744.
- [44] M. Babokhov, K. Hibino, Y. Itoh, K. Maeshima, *J. Mol. Biol.* **2019**, <https://doi.org/10.1016/j.jmb.2019.10.018>.
- [45] K. Maeshima, K. Kaizu, S. Tamura, T. Nozaki, T. Kokubo, K. Takahashi, *J. Phys.: Condens. Matter* **2015**, *27*, 064116.
- [46] M. Cremer, V. J. Schmid, F. Kraus, Y. Markaki, I. Hellmann, A. Maiser, H. Leonhardt, S. John, J. Stamatoyannopoulos, T. Cremer, *Epigenet. Chromatin* **2017**, *10*, 39.
- [47] M. Cremer, T. Cremer, *Genes, Chromosomes Cancer* **2019**, *58*, 427.
- [48] T. Cremer, G. Kreth, H. Koester, R. H. Fink, R. Heintzmann, M. Cremer, I. Solovei, D. Zink, C. Cremer, *Crit. Rev. Eukaryot. Gene Expr.* **2000**, *10*, 38.
- [49] U. Wehrli, *Tidying Up Art*, Prestel, New York **2003**.
- [50] R. Hancock, *Biochemistry* **2018**, *83*, 326.
- [51] B. Deplancke, D. Alpern, V. Gardeux, *Cell* **2016**, *166*, 538.
- [52] J. De Las Rivas, C. Fontanillo, *PLoS Comput. Biol.* **2010**, *6*, e1000807.
- [53] S. E. A. Ozbabacan, H. B. Engin, A. Gursoy, O. Keskin, *Protein Eng., Des. Sel.* **2011**, *24*, 635.
- [54] F. J. Blanco, G. Montoya, *FEBS J.* **2011**, *278*, 1643.
- [55] J. A. Croft, J. M. Bridger, S. Boyle, P. Perry, P. Teague, W. A. Bickmore, *J. Cell Biol.* **1999**, *145*, 1119.
- [56] S. Boyle, S. Gilchrist, J. M. Bridger, N. L. Mahy, J. A. Ellis, W. A. Bickmore, *Hum. Mol. Genet.* **2001**, *10*, 211.
- [57] M. Cremer, J. von Hase, T. Volm, A. Brero, G. Kreth, J. Walter, C. Fischer, I. Solovei, C. Cremer, T. Cremer, *Chromosome Res.* **2001**, *9*, 541.
- [58] F. A. Habermann, M. Cremer, J. Walter, G. Kreth, J. von Hase, K. Bauer, J. Wienberg, C. Cremer, T. Cremer, I. Solovei, *Chromosome Res.* **2001**, *9*, 569.
- [59] H. Tanabe, F. A. Habermann, I. Solovei, M. Cremer, T. Cremer, *Mutat. Res., Fundam. Mol. Mech. Mutagen.* **2002**, *504*, 37.
- [60] K. Kupper, A. Kolbl, D. Biener, S. Dittrich, J. von Hase, T. Thormeyer, H. Fiegler, N. P. Carter, M. R. Speicher, T. Cremer, M. Cremer, *Chromosoma* **2007**, *116*, 285.
- [61] M. Neusser, V. Schubel, A. Koch, T. Cremer, S. Muller, *Chromosoma* **2007**, *116*, 307.
- [62] T. Szczepinska, A. M. Rusek, D. Plewczynski, *Genes, Chromosomes Cancer* **2019**, *58*, 500.
- [63] M. Narita, S. Nunez, E. Heard, M. Narita, A. W. Lin, S. A. Hearn, D. L. Spector, G. J. Hannon, S. W. Lowe, *Cell* **2003**, *113*, 703.
- [64] D. Illner, R. Zinner, V. Handtke, J. Rouquette, H. Strickfaden, C. Lanctot, M. Conrad, A. Seiler, A. Imhof, T. Cremer, M. Cremer, *Exp. Cell Res.* **2010**, *316*, 1662.
- [65] T. Chandra, K. Kirschner, J. Y. Thuret, B. D. Pope, T. Ryba, S. Newman, K. Ahmed, S. A. Samarajiwa, R. Salama, T. Carroll, R. Stark, R. Janky, M. Narita, L. Xue, A. Chicas, S. Nunez, R. Janknecht, Y. Hayashi-Takanaka, M. D. Wilson, A. Marshall, D. T. Odom, M. M. Babu, D. P. Bazett-Jones, S. Tavare, P. A. Edwards, S. W. Lowe, H. Kimura, D. M. Gilbert, M. Narita, *Mol. Cell* **2012**, *47*, 203.
- [66] T. Chandra, P. A. Ewels, S. Schoenfelder, M. Furlan-Magaril, S. W. Wingett, K. Kirschner, J. Y. Thuret, S. Andrews, P. Fraser, W. Reik, *Cell Rep.* **2015**, *10*, 471.
- [67] M. R. Branco, A. Pombo, *PLoS Biol.* **2006**, *4*, e138.
- [68] H. Albiez, M. Cremer, C. Tiberi, L. Vecchio, L. Schermelleh, S. Dittrich, K. Kupper, B. Joffe, T. Thormeyer, J. von Hase, S. Yang, K. Rohr,



- H. Leonhardt, I. Solovei, C. Cremer, S. Fakan, T. Cremer, *Chromosome Res.* **2006**, *14*, 707.
- [69] A. Bolzer, G. Kreth, I. Solovei, D. Koehler, K. Saracoglu, C. Fauth, S. Muller, R. Eils, C. Cremer, M. R. Speicher, T. Cremer, *PLoS Biol.* **2005**, *3*, e157.
- [70] A. L. Dounce, *Am. Sci.* **1971**, *59*, 74.
- [71] F. Guilak, J. R. Tedrow, R. Burgkart, *Biochem. Biophys. Res. Commun.* **2000**, *269*, 781.
- [72] F. Erdel, M. Baum, K. Rippe, *J. Phys.: Condens. Matter* **2015**, *27*, 064115.
- [73] H. Strickfaden, A. Zunhammer, S. van Koningsbruggen, D. Kohler, T. Cremer, *Nucleus* **2010**, *1*, 284.
- [74] D. Smeets, Y. Markaki, V. J. Schmid, F. Kraus, A. Tattermusch, A. Cerase, M. Sterr, S. Fiedler, J. Demmerle, J. Popken, H. Leonhardt, N. Brockdorff, T. Cremer, L. Schermelleh, M. Cremer, *Epigenet. Chromatin* **2014**, *7*, 8.
- [75] I. Kirmes, A. Szczurek, K. Prakash, I. Charapitsa, C. Heiser, M. Musheev, F. Schock, K. Fornalczyk, D. Ma, U. Birk, C. Cremer, G. Reid, *Genome Biol.* **2015**, *16*, 246.
- [76] I. S. Mehta, M. Amira, J. H. Harvey, J. M. Bridger, *Genome Biol.* **2010**, *11*, R5.
- [77] M. Falk, Y. Feodorova, N. Naumova, M. Imakaev, B. R. Lajoie, H. Leonhardt, B. Joffe, J. Dekker, G. Fudenberg, I. Solovei, L. A. Mirny, *Nature* **2019**, *570*, 395.
- [78] E. Ruska, *Biosci. Rep.* **1987**, *7*, 607.
- [79] A. Monneron, W. Bernhard, *J. Ultrastruct. Res.* **1969**, *27*, 266.
- [80] S. Fakan, W. Bernhard, *Exp. Cell Res.* **1971**, *67*, 129.
- [81] P. Petrov, W. Bernhard, *J. Ultrastruct. Res.* **1971**, *35*, 386.
- [82] S. Fakan, W. Bernhard, *Exp. Cell Res.* **1973**, *79*, 431.
- [83] D. Cmarko, P. J. Verschure, T. E. Martin, M. E. Dahmus, S. Krause, X. D. Fu, R. van Driel, S. Fakan, *Mol. Biol. Cell* **1999**, *10*, 211.
- [84] J. Niedojadlo, C. Perret-Vivancos, K. H. Kalland, D. Cmarko, T. Cremer, R. van Driel, S. Fakan, *Exp. Cell Res.* **2011**, *317*, 433.
- [85] S. Fakan, R. Hancock, *Exp. Cell Res.* **1974**, *83*, 95.
- [86] F. Jaunin, A. E. Visser, D. Cmarko, J. A. Aten, S. Fakan, *Exp. Cell Res.* **2000**, *260*, 313.
- [87] C. Kizilyaprak, J. Daraspe, B. M. Humbel, *J. Microsc.* **2014**, *254*, 109.
- [88] Q. He, M. Hsueh, G. Zhang, D. C. Joy, R. D. Leapman, *Sci. Rep.* **2018**, *8*, 12985.
- [89] J. Rouquette, C. Genoud, G. H. Vazquez-Nin, B. Kraus, T. Cremer, S. Fakan, *Chromosome Res.* **2009**, *17*, 801.
- [90] T. V. Hoang, C. Kizilyaprak, D. Spehner, B. M. Humbel, P. Schultz, *J. Struct. Biol.* **2017**, *197*, 123.
- [91] D. P. Bazett-Jones, M. J. Hendzel, *Methods* **1999**, *17*, 188.
- [92] H. Strickfaden, A. K. Sharma, M. J. Hendzel, *bioRxiv* 541086 **2019**.
- [93] J. J. Landry, P. T. Pyl, T. Rausch, T. Zichner, M. M. Tekkedil, A. M. Stutz, A. Jauch, R. S. Aiyar, G. Pau, N. Delhomme, J. Gagneur, J. O. Korbel, W. Huber, L. M. Steinmetz, *G3: Genes, Genomes, Genetics* **2013**, *3*, 1213.
- [94] X. Shu, V. Lev-Ram, T. J. Deerinck, Y. Qi, E. B. Ramko, M. W. Davidson, Y. Jin, M. H. Ellisman, R. Y. Tsien, *PLoS Biol.* **2011**, *9*, e1001041.
- [95] A. S. Kovarikova, S. Legartova, J. Krejci, E. Bartova, *Aging* **2018**, *10*, 2585.
- [96] H. D. Ou, S. Phan, T. J. Deerinck, A. Thor, M. H. Ellisman, C. C. O'Shea, *Science* **2017**, *357*, eaag0025.
- [97] M. A. Ricci, C. Manzo, M. F. Garcia-Parajo, M. Lakadamyali, M. P. Cosma, *Cell* **2015**, *160*, 1145.
- [98] A. Esposito, C. Annunziatella, S. Bianco, A. M. Chiariello, L. Fiorillo, M. Nicodemi, *Wiley Interdiscip. Rev.: Syst. Biol. Med.* **2019**, *11*, e1444.
- [99] M. A. Le Gros, E. J. Clowney, A. Magklara, A. Yen, E. Markenscoff-Papadimitriou, B. Colquitt, M. Myllys, M. Kellis, S. Lomvardas, C. A. Larabell, *Cell Rep.* **2016**, *17*, 2125.
- [100] A. Ekman, J. H. Chen, V. Weinhardt, M. Do, G. McDermott, M. A. Le Gros, C. A. Larabell, *Synchrotron Light Sources and Free-Electron Lasers* (Eds: E. J. Jaeschke, S. Khan, J. R. Schneider, J. B. Hastings), Springer Nature, Cham, Switzerland **2019**, pp. 1–32.
- [101] D. P. Hoffman, G. Shtengel, C. S. Xu, K. R. Campbell, M. Freeman, L. Wang, D. Milkie, H. A. Pasolli, N. Iyer, J. A. Bogovic, D. R. Stabley, A. Shirinifard, S. Pang, D. Peale, K. Schaefer, W. Pomp, C. Chang, J. Lippincott-Schwartz, T. Kirchhausen, D. J. Solecki, E. Betzig, H. F. Hess, *bioRxiv* **2019**, 773986.
- [102] L. Schermelleh, P. M. Carlton, S. Haase, L. Shao, L. Winoto, P. Kner, B. Burke, M. C. Cardoso, D. A. Agard, M. G. Gustafsson, H. Leonhardt, J. W. Sedat, *Science* **2008**, *320*, 1332.
- [103] C. Cremer, B. R. Masters, *Eur. Phys. J. H* **2013**, *38*, 281.
- [104] M. Ehrenberg, *R. Swed. Acad. Eng. Sci.* **2014**.
- [105] L. Schermelleh, A. Ferrand, T. Huser, C. Eggeling, M. Sauer, O. Biehlmaier, G. P. C. Drummen, *Nat. Cell Biol.* **2019**, *21*, 72.
- [106] S. W. Hell, J. Wichmann, *Opt. Lett.* **1994**, *19*, 780.
- [107] S. W. Hell, *Science* **2007**, *316*, 1153.
- [108] R. Heintzmann, C. Cremer, *SPIE Proc.* **1999**, *3568*, 336833.
- [109] M. G. Gustafsson, *J. Microsc.* **2000**, *198*, 82.
- [110] R. Heintzmann, T. Huser, *Chem. Rev.* **2017**, *117*, 13890.
- [111] K. A. Lidke, B. Rieger, T. M. Jovin, R. Heintzmann, *Opt. Express* **2005**, *13*, 7052.
- [112] E. Betzig, G. H. Patterson, R. Sougrat, O. W. Lindwasser, S. Olenych, J. S. Bonifacino, M. W. Davidson, J. Lippincott-Schwartz, H. F. Hess, *Science* **2006**, *313*, 1642.
- [113] M. J. Rust, M. Bates, X. Zhuang, *Nat. Methods* **2006**, *3*, 793.
- [114] A. Esa, P. Edelmann, G. Kreth, L. Trakhtenbrot, N. Amariglio, G. Rechavi, M. Hausmann, C. Cremer, *J. Microsc.* **2000**, *199*, 96.
- [115] R. M. Dickson, A. B. Cubitt, R. Y. Tsien, W. E. Moerner, *Nature* **1997**, *388*, 355.
- [116] J. Reymann, D. Baddeley, M. Gunkel, P. Lemmer, W. Stadter, T. Jegou, K. Rippe, C. Cremer, U. Birk, *Chromosome Res.* **2008**, *16*, 367.
- [117] P. Lemmer, M. Gunkel, Y. Weiland, P. Muller, D. Baddeley, R. Kaufmann, A. Urich, H. Eipel, R. Amberger, M. Hausmann, C. Cremer, *J. Microsc.* **2009**, *235*, 163.
- [118] A. Szczurek, L. Klewes, J. Xing, A. Gourram, U. Birk, H. Knecht, J. W. Dobrucki, S. Mai, C. Cremer, *Nucleic Acids Res.* **2017**, *45*, D56.
- [119] C. Cremer, A. Szczurek, F. Schock, A. Gourram, U. Birk, *Methods* **2017**, *123*, 11.
- [120] U. J. Birk, *Genes* **2019**, *10*, e493.
- [121] Y. Markaki, M. Gunkel, L. Schermelleh, S. Beichmanis, J. Neumann, M. Heidemann, H. Leonhardt, D. Eick, C. Cremer, T. Cremer, *Cold Spring Harbor Symp. Quant. Biol.* **2010**, *75*, 475.
- [122] Y. Markaki, D. Smeets, S. Fiedler, V. J. Schmid, L. Schermelleh, T. Cremer, M. Cremer, *BioEssays* **2012**, *34*, 412.
- [123] B. Hubner, M. Lomiento, F. Mammoli, D. Illner, Y. Markaki, S. Ferrari, M. Cremer, T. Cremer, *Epigenet. Chromatin* **2015**, *8*, 47.
- [124] M. Cremer, K. Brandstetter, S. Maiser, S. S. P. Rao, V. J. Schmid, N. Mitra, S. Mamberti, K. N. Klein, D. M. Gilbert, H. Leonhardt, M. C. Cardoso, E. Lieberman-Aiden, H. Harz, T. Cremer, *bioRxiv* **2019**, 816611.
- [125] E. Miron, R. Oldenkamp, D. M. S. Pinto, J. M. Brown, A. R. Faria, H. A. Shaban, J. D. P. Rhodes, C. Innocent, S. de Ornellas, V. Buckle, L. Schermelleh, *bioRxiv* **2019**, 566638.
- [126] V. J. Schmid, M. Cremer, T. Cremer, *Methods* **2017**, *123*, 33.
- [127] A. Malhas, C. Goulbourne, D. J. Vaux, *Trends Cell Biol.* **2011**, *21*, 362.
- [128] J. Popken, A. Graf, S. Krebs, H. Blum, V. J. Schmid, A. Strauss, T. Guengoer, V. Zakhartchenko, E. Wolf, T. Cremer, *PLoS One* **2015**, *10*, e0124619.
- [129] J. Kind, L. Pagie, H. Ortazokoyun, S. Boyle, S. S. de Vries, H. Janssen, M. Amendola, L. D. Nolen, W. A. Bickmore, B. van Steensel, *Cell* **2013**, *153*, 178.
- [130] B. van Steensel, A. S. Belmont, *Cell* **2017**, *169*, 780.
- [131] A. Vivante, E. Brozgol, I. Bronshtein, V. Levi, Y. Garini, *Genes, Chromosomes Cancer* **2019**, *58*, 437.

- [132] R. S. Nozawa, L. Boteva, D. C. Soares, C. Naughton, A. R. Dun, A. Buckle, B. Ramsahoye, P. C. Bruton, R. S. Saleeb, M. Arnedo, B. Hill, R. R. Duncan, S. K. Maciver, N. Gilbert, *Cell* **2017**, *169*, 1214.
- [133] S. V. Razin, O. V. Iarovaia, Y. S. Vassetzky, *Chromosoma* **2014**, *123*, 217.
- [134] R. Berezney, M. J. Mortillaro, H. Ma, X. Wei, J. Samarabandu, *Int. Rev. Cytol.* **1995**, *162A*, 1.
- [135] N. Naetar, S. Ferraioli, R. Foisner, *J. Cell Sci.* **2017**, *130*, 2087.
- [136] C. Uhler, G. V. Shivashankar, *Nat. Rev. Mol. Cell Biol.* **2017**, *18*, 717.
- [137] P. M. Diesinger, D. W. Heermann, *Phys. Rev. E* **2006**, *74*, 031904.
- [138] J. Langowski, *Eur. Phys. J. E* **2006**, *19*, 241.
- [139] K. Prakash, D. Fournier, *Biosystems* **2018**, *164*, 49.
- [140] M. Eltsov, K. M. Maclellan, K. Maeshima, A. S. Frangakis, J. Dubochet, *Proc. Natl. Acad. Sci. USA* **2008**, *105*, 19732.
- [141] E. Fussner, R. W. Ching, D. P. Bazett-Jones, *Trends Biochem. Sci.* **2011**, *36*, 1.
- [142] K. Maeshima, S. Hihara, M. Eltsov, *Curr. Opin. Cell Biol.* **2010**, *22*, 291.
- [143] K. Maeshima, R. Rogge, S. Tamura, Y. Joti, T. Hikima, H. Szerlong, C. Krause, J. Herman, E. Seidel, J. DeLuca, T. Ishikawa, J. C. Hansen, *EMBO J.* **2016**, *35*, 1115.
- [144] K. Maeshima, R. Imai, S. Tamura, T. Nozaki, *Chromosoma* **2014**, *123*, 225.
- [145] S. Martin, A. V. Failla, U. Spori, C. Cremer, A. Pombo, *Mol. Biol. Cell* **2004**, *15*, 2449.
- [146] D. Baddeley, V. O. Chagin, L. Schermelleh, S. Martin, A. Pombo, P. M. Carlton, A. Gahl, P. Domaing, U. Birk, H. Leonhardt, C. Cremer, M. C. Cardoso, *Nucleic Acids Res.* **2010**, *38*, e8.
- [147] R. Nagashima, K. Hibino, S. S. Ashwin, M. Babokhov, S. Fujishiro, R. Imai, T. Nozaki, S. Tamura, T. Tani, H. Kimura, M. Shribak, M. T. Kanemaki, M. Sasai, K. Maeshima, *J. Cell Biol.* **2019**, *218*, 1511.
- [148] S. M. Gorisch, M. Wachsmuth, K. F. Toth, P. Lichter, K. Rippe, *J. Cell Sci.* **2005**, *118*, 5825.
- [149] M. Wachsmuth, T. A. Knoch, K. Rippe, *Epigenet. Chromatin* **2016**, *9*, 57.
- [150] A. R. Strom, A. V. Emelyanov, M. Mir, D. V. Fyodorov, X. Darzacq, G. H. Karpen, *Nature* **2017**, *547*, 241.
- [151] M. J. Rowley, V. G. Corces, *Nat. Rev. Genet.* **2018**, *19*, 789.
- [152] H. Strickfaden, K. Missiaen, M. Hendzel, U. Underhill *bioRxiv*, **2019**, 776625.
- [153] E. Dolgin, *Nature* **2018**, *555*, 300.
- [154] R. Imai, T. Nozaki, T. Tani, K. Kaizu, K. Hibino, S. Ide, S. Tamura, K. Takahashi, M. Shribak, K. Maeshima, *Mol. Biol. Cell* **2017**, *28*, 3349.
- [155] E. Lieberman-Aiden, N. L. van Berkum, L. Williams, M. Imakaev, T. Ragoczy, A. Telling, I. Amit, B. R. Lajoie, P. J. Sabo, M. O. Dorschner, R. Sandstrom, B. Bernstein, M. A. Bender, M. Groudine, A. Gnirke, J. Stamatoyannopoulos, L. A. Mirny, E. S. Lander, J. Dekker, *Science* **2009**, *326*, 289.
- [156] J. R. Dixon, D. U. Gorkin, B. Ren, *Mol. Cell* **2016**, *62*, 668.
- [157] Q. Szabo, D. Jost, J. M. Chang, D. I. Cattoni, G. L. Papadopoulos, B. Bonev, T. Sexton, J. Gurgu, C. Jacquier, M. Nollmann, F. Bantignies, G. Cavalli, *Sci. Adv.* **2018**, *4*, eaar8082.
- [158] M. J. Fullwood, M. H. Liu, Y. F. Pan, J. Liu, H. Xu, Y. B. Mohamed, Y. L. Orlov, S. Velkov, A. Ho, P. H. Mei, E. G. Y. Chew, P. Y. H. Huang, W.-J. Welboren, Y. Han, H. S. Ooi, P. N. Ariyaratne, V. B. Vega, Y. Luo, P. Y. Tan, P. Y. Choy, K. D. S. A. Wansa, B. Zhao, K. S. Lim, S. C. Leow, J. S. Yow, R. Joseph, H. Li, K. V. Desai, J. S. Thomsen, Y. K. Lee, R. K. M. Karuturi, T. Herve, G. Bourque, H. G. Stunnenberg, X. Ruan, V. Cacheux-Rataboul, W.-K. Sung, E. T. Liu, C.-L. Wei, E. Cheung, Y. Ruan, *Nature* **2009**, *462*, 58.
- [159] S. Fu, L. Zhang, J. Lv, B. Zhu, W. Wang, X. Wang, *Semin. Cell Dev. Biol.* **2019**, *90*, 43.
- [160] R. A. Beagrie, A. Scialdone, M. Schueler, D. C. Kraemer, M. Chotalia, S. Q. Xie, M. Barbieri, I. de Santiago, L. M. Lavitas, M. R. Branco, J. Fraser, J. Dostie, L. Game, N. Dillon, P. A. Edwards, M. Nicodemi, A. Pombo, *Nature* **2017**, *543*, 519.
- [161] J. Paulsen, T. M. L. Ali, P. Collas, *Nat. Protoc.* **2018**, *13*, 1137.
- [162] T. Cremer, M. Cremer, *Cold Spring Harbor Perspect. Biol.* **2010**, *2*, a003889.
- [163] S. S. Rao, M. H. Huntley, N. C. Durand, E. K. Stamenova, I. D. Bochkov, J. T. Robinson, A. L. Sanborn, I. Machol, A. D. Omer, E. S. Lander, E. L. Aiden, *Cell* **2014**, *159*, 1665.
- [164] B. Bintu, L. J. Mateo, J. H. Su, N. A. Sinnott-Armstrong, M. Parker, S. Kinrot, K. Yamaya, A. N. Boettiger, X. Zhuang, *Science* **2018**, *362*, eaau1783.
- [165] T. Nozaki, R. Imai, M. Tanbo, R. Nagashima, S. Tamura, T. Tani, Y. Joti, M. Tomita, K. Hibino, M. T. Kanemaki, K. S. Wendt, Y. Okada, T. Nagai, K. Maeshima, *Mol. Cell* **2017**, *67*, 282.
- [166] H. A. Shaban, R. Barth, K. Bystricky, *Nucleic Acids Res.* **2018**, *46*, e77.
- [167] R. Barth, K. Bystricky, H. A. Shaban, *bioRxiv* **2019**, 777482.
- [168] J. Xu, Y. Liu, *FEBS J.* **2019**, *286*, 3095.
- [169] H. Bornfleth, P. Edelmann, D. Zink, T. Cremer, C. Cremer, *Biophys. J.* **1999**, *77*, 2871.
- [170] H. Ma, L. C. Tu, A. Naseri, M. Huisman, S. Zhang, D. Grunwald, T. Pederson, *Nat. Biotechnol.* **2016**, *34*, 528.
- [171] Z. Liu, R. Tjian, *J. Cell Biol.* **2018**, *217*, 1181.
- [172] S. Shao, B. Xue, Y. Sun, *Biophys. J.* **2018**, *115*, 181.
- [173] A. Regev, S. A. Teichmann, E. S. Lander, I. Amit, C. Benoist, E. Birney, B. Bodenmiller, P. Campbell, P. Carninci, M. Clatworthy, H. Clevers, B. Deplancke, I. Dunham, J. Eberwine, R. Eils, W. Enard, A. Farmer, L. Fugger, B. Gottgens, N. Hacohen, M. Haniffa, M. Hemberg, S. Kim, P. Klenerman, A. Kriegstein, E. Lein, S. Linnarsson, E. Lundberg, J. Lundeberg, P. Majumder, J. C. Marioni, M. Merad, M. Mhlanga, M. Nawijn, M. Netea, G. Nolan, D. Pe'er, A. Phillipakis, C. P. Ponting, S. Quake, W. Reik, O. Rozenblatt-Rosen, J. Sanes, R. Satija, T. N. Schumacher, A. Shalek, E. Shapiro, P. Sharma, J. W. Shin, O. Stegle, M. Stratton, M. J. T. Stubbington, F. J. Theis, M. Uhlen, A. van Oudenaarden, A. Wagner, F. Watt, J. Weissman, B. Wold, R. Xavier, N. Yosef, Human Cell Atlas meeting participants, *eLife* **2017**, *6*, e27041.
- [174] D. A. Cusanovich, A. J. Hill, D. Aghamirzaie, R. M. Daza, H. A. Pliner, J. B. Berletch, G. N. Filippova, X. Huang, L. Christiansen, W. S. DeWitt, C. Lee, S. G. Regalado, D. F. Read, F. J. Steemers, C. M. Distechte, C. Trapnell, J. Shendure, *Cell* **2018**, *174*, 1309.
- [175] B. K. Kragestein, M. Spielmann, C. Paliou, V. Heinrich, R. Schopflin, A. Esposito, C. Annunziatella, S. Bianco, A. M. Chiariello, I. Jerkovic, I. Harabula, P. Guckelberger, M. Pechstein, L. Wittler, W. L. Chan, M. Franke, D. G. Lupianez, K. Kraft, B. Timmermann, M. Vingron, A. Visel, M. Nicodemi, S. Mundlos, G. Andrey, *Nat. Genet.* **2018**, *50*, 1463.
- [176] J. Cao, M. Spielmann, X. Qiu, X. Huang, D. M. Ibrahim, A. J. Hill, F. Zhang, S. Mundlos, L. Christiansen, F. J. Steemers, C. Trapnell, J. Shendure, *Nature* **2019**, *566*, 496.